Report No. K-TRAN: KSU-21-6 ▪ FINAL REPORT ▪ July 2022

Probabilistic Wind Speed Model for Local Data in All Kansas Counties

Khalid W. Al Shboul, M.Sc.
Hayder A. Rasheed, Ph.D., P.E., F.ASCE, F.ACI, F.SEI

Kansas State University Transportation Center

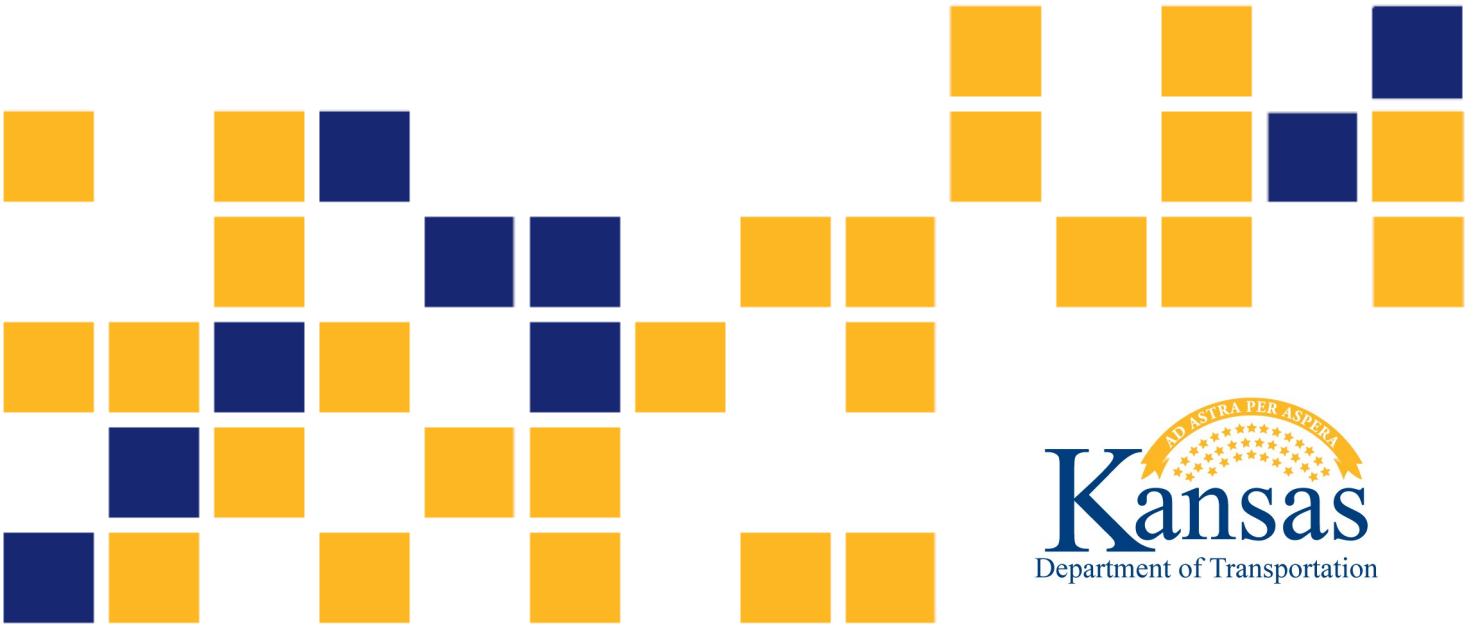

Kansas
Department of Transportation

1 Report No. K-TRAN: KSU-21-6	**2 Government Accession No.**	**3 Recipient Catalog No.**
4 Title and Subtitle Probabilistic Wind Speed Model for Local Data in All Kansas Counties		**5 Report Date** July 2022 **6 Performing Organization Code**
7 Author(s) Khalid W. Al Shboul, M.Sc.; Hayder A. Rasheed, Ph.D., P.E., F.ASCE, F.ACI, F.SEI		**8 Performing Organization Report No.**
9 Performing Organization Name and Address Kansas State University Transportation Center Department of Civil Engineering 2118 Fiedler Hall 1701C Platt Street Manhattan, KS 66506-5000		**10 Work Unit No. (TRAIS)** **11 Contract or Grant No.** C2166
12 Sponsoring Agency Name and Address Kansas Department of Transportation Bureau of Research 2300 SW Van Buren Topeka, Kansas 66611-1195		**13 Type of Report and Period Covered** Final Report August 2020–March 2022 **14 Sponsoring Agency Code** RE-0811-01

15 Supplementary Notes
For more information write to address in block 9.

16 Abstract

This study developed a spatial interpolation technique using finite element shape functions to derive wind speed records for all unsampled Kansas counties from data recorded at 17 city locations in and near Kansas. A computational method using the Kaimal spectrum is presented for generating artificial time histories of wind speeds. This is done to extract wind-cycle distribution using the Rainflow counting technique, which can be used as input for fatigue analysis procedures for highway sign structures. The predeveloped wind speed-cycle database was extended into the future to allow fatigue inspection over the service life of the sign structures. A user-friendly software was designed using C# to interpolate wind-speed cycles for all Kansas counties. This software is expected to facilitate fatigue-life inspection because it generates a wind-loading output file that can be used for other fatigue-life simulators (e.g., cantilever sign structures and butterfly sign structure simulators).

17 Key Words Wind, Interpolation, Signs, Database, Structural health monitoring		**18 Distribution Statement** No restrictions. This document is available to the public through the National Technical Information Service www.ntis.gov.	
19 Security Classification (of this report) Unclassified	**20 Security Classification (of this page)** Unclassified	**21 No. of pages** 72	**22 Price**

Form DOT F 1700.7 (8-72)

This page intentionally left blank.

Probabilistic Wind Speed Model for Local Data in All Kansas Counties

Final Report

Prepared by

Khalid W. Al Shboul, M.Sc.
Hayder A. Rasheed, Ph.D., P.E., F.ASCE, F.ACI, F.SEI

Kansas State University Transportation Center

A Report on Research Sponsored by

THE KANSAS DEPARTMENT OF TRANSPORTATION
TOPEKA, KANSAS

and

KANSAS STATE UNIVERSITY TRANSPORTATION CENTER
MANHATTAN, KANSAS

July 2022

PREFACE

The Kansas Department of Transportation's (KDOT) Kansas Transportation Research and New-Developments (K-TRAN) Research Program funded this research project. It is an ongoing, cooperative and comprehensive research program addressing transportation needs of the state of Kansas utilizing academic and research resources from KDOT, Kansas State University and the University of Kansas. Transportation professionals in KDOT and the universities jointly develop the projects included in the research program.

NOTICE

The authors and the state of Kansas do not endorse products or manufacturers. Trade and manufacturers names appear herein solely because they are considered essential to the object of this report.

This information is available in alternative accessible formats. To obtain an alternative format, contact the Office of Public Affairs, Kansas Department of Transportation, 700 SW Harrison, 2nd Floor – West Wing, Topeka, Kansas 66603-3745 or phone (785) 296-3585 (Voice) (TDD).

DISCLAIMER

The contents of this report reflect the views of the authors who are responsible for the facts and accuracy of the data presented herein. The contents do not necessarily reflect the views or the policies of the state of Kansas. This report does not constitute a standard, specification or regulation.

Abstract

This study developed a spatial interpolation technique using finite element shape functions to derive wind speed records for all unsampled Kansas counties from data recorded at 17 city locations in and near Kansas. A computational method using the Kaimal spectrum is presented for generating artificial time histories of wind speeds. This is done to extract wind-cycle distribution using the Rainflow counting technique, which can be used as input for fatigue analysis procedures for highway sign structures. The predeveloped wind speed-cycle database was extended into the future to allow fatigue inspection over the service life of the sign structures. A user-friendly software was designed using C# to interpolate wind-speed cycles for all Kansas counties. This software is expected to facilitate fatigue-life inspection because it generates a wind-loading output file that can be used for other fatigue-life simulators (e.g., cantilever sign structures and butterfly sign structure simulators).

Acknowledgments

This research was made possible by funding from the Kansas Department of Transportation's (KDOT) Kansas Transportation Research and New-Developments (K-TRAN) Program. Thanks are extended to the KDOT team members in the Bureau of Structures and Geotechnical Services that supported the project during all its development stages. Special thanks are extended to Karen Peterson, Eric Anderson, and Mark Hurt.

Table of Contents

List of Tables

List of Figures

Chapter 1: Introduction

1.1 Overview

Quantification of wind loading is a crucial stage in the design of engineering structures prone to wind. Wind loading typically focuses on the strongest winds or extreme wind speeds that occur during a structure's lifetime. Robust wind structural analysis and design require an accurate estimation of extreme wind-speed values and wind-speed variations over time. Although wind behavior is assumed to be a stochastic process, many researchers have attempted to model and simulate its behavior over time. Metrological stations are usually distributed over various locations to record wind-speed values, and extreme wind speeds are estimated from these records. However, it is impractical to distribute and set up metrological stations everywhere. For uncovered geographical areas, wind-speed records can be spatially interpolated from measured areas. In addition, metrological stations report averaged wind speeds over time and peak wind-speed values, without recording instantaneous wind-speed measurements. For accurate engineering design, wind-time profiles should be artificially generated.

1.2 Objectives

Full-span overhead sign support structures are critical ancillary systems that use a set of mounted highway signs to guide drivers. The Kansas Department of Transportation (KDOT) also utilizes cantilevered and butterfly structures in their transportation system. To prevent possible hazards that may result from fatigue damage, a frequent comprehensive evaluation of these structures should be made. The critical factor that enhances the inspection accuracy of these structures is accurate quantification of the wind-loading scenarios that structures may experience during their lifetime. This project pursued the following objectives:

1. Develop a detailed spatial wind-speed interpolation using finite element (FE) shape functions to provide wind-speed records for all counties in Kansas.
2. Derive daily wind-time profiles for the 45 years used in this study (1975–2019).

3. Carry out Rainflow analysis of these time histories to provide a descriptive wind-loading scenario in terms of the number of cycles.
4. Ensure this wind-speed data set is projectable into the future by mirroring the data from the end of December 2019 / beginning of January 2020 timeline.

1.3 Scope

This report includes a total of seven chapters. The first chapter provides a general introduction to the project, and the second chapter presents a brief literature review relevant to topics addressed by this report. Chapter 3 includes a detailed formulation of the finite element spatial interpolation and development of the wind-histories records. Chapter 4 details procedures for the development of the Wind-Cycle generator software. Chapter 5 describes the results and discusses the finding of the analyses, while Chapter 6 provides an assessment and validation of the developed procedures. Chapter 7 draws necessary conclusions and presents recommendations.

Chapter 2: Literature Review

2.1 Overview

Sign support structures are considered critical ancillary systems, which are essential components of the highway infrastructure, to guide commuters. Fatigue response due to wind-loading should be monitored and analyzed to predict remaining structural fatigue life to prevent damage or failure. Wind turbulence must also be considered in structural engineering loading applications because some structures may exhibit resonant responses produced by velocity fluctuations of wind turbulency. In addition, the aerodynamic behavior of a structure may be highly dependent upon airflow turbulence. Therefore, wind simulations generated during structural analysis must accurately capture the characteristics of natural turbulent wind. Unfortunately, however, because wind is dynamic in nature, the accurate estimation of turbulent wind characteristics during any wind event is cumbersome. These processes may not be stationary (Kattan, 2003; Ginal, 2003).

2.2 Analytical Modeling of Natural Wind

The literature has investigated several techniques to model the power spectral density function for turbulent wind speed in practical engineering applications. Davenport (1962) used approximately 70 spectra results of horizontal components of gust in intense wind events in various locations and circumstances worldwide. Accordingly, he proposed Equation 2.1. Because the Davenport model is independent of height above the ground surface, turbulence in the generated time history is fixed to a certain mean velocity at a particular reference height. In high-rise structures, this height may not coincide with the structure's height under investigation, so the effect of height on mean wind speed should be introduced.

$$S_D(n) = 4kV_{10}^2 \frac{x^2}{n(1+x^2)^{4/3}}$$

Equation 2.1

$$x = 1200\frac{n}{V_{10}}$$

Equation 2.2

$$V(z) = V_{10}.(\frac{Z}{10})^{\alpha}$$

Equation 2.3

Where:

$S_D(n)$ is the fluctuation wind-speed spectrum;

n is the frequency;

z is the height;

$V(z)$ is the mean wind speed at the height of z;

V_{10} is the mean wind speed at the standard height of 10 m;

α is the ground roughness exponent; and

k is the terrain roughness factor.

Kaimal et al. (1972) proposed modifications to the Davenport model to account for structural height above the ground and suggested the following empirical formula (Equation 2.4) to simulate the power spectral density. The Kaimal spectrum includes the effect of height on turbulent wind. Kaimal spectrum has proven to be accurate in the high frequency range in which most engineered structures respond.

$$S_K(f) = \frac{200U_*^2 z}{U_z(1 + 50\frac{fz}{U_z})^{5/3}}$$

Equation 2.4

$$U_* = \sqrt{\frac{\sigma_u^2}{6}}$$

Equation 2.5

$$\sigma_u^2 = 6KU_z^2$$

Equation 2.6

Where:

S_K is the Kaimal spectrum,

z is the height above the ground,

$U_*$is the shear velocity,

U_z is the mean wind velocity at z, and

f is the specified frequency.

2.3 Spatial Variation and Interpolation of Wind Speeds

Weather data are generally recorded at specific locations, but spatial interpolation can be used to estimate wind speed values at other locations. Various deterministic and geostatistical interpolation methods can approximate values for spatially continuous phenomena from measured values at limited sample points. Most spatial interpolation techniques are based on the concept that derived values are represented as the weighted average of measured values at the sample points. The general interpolation formula is

$$\acute{Z}\,(x_\circ, y_\circ) = \sum_{i=1}^{n} w_i\, Z(x_i, y_i)$$

Equation 2.7

Where:

$\acute{Z}\,(x_\circ, y_\circ)$ represents the predicated value at a specific location,

$(x_\circ, y_\circ)$, $Z(x_i, y_i)$ represents the measured value at the sample point,

(x_i, y_i), w_i is the weight assigned to the sample point, and

n is the number of sampling points used in the interpolation (Luo et al., 2008; Webster & Oliver, 2007).

Chapter 3: Formulation

The framework for developing the wind-cycle database for all Kansas counties requires wind-speed data for the entire 45-year timespan under investigation. A deterministic spatial interpolation technique using finite element shape functions was used to build a comprehensive 45-year database of high and mean wind speeds. Kansas was divided into twelve geometrical interpolation zones to cover the entire domain, combined with quadrilateral and triangular shapes, as shown in Figure 3.1.

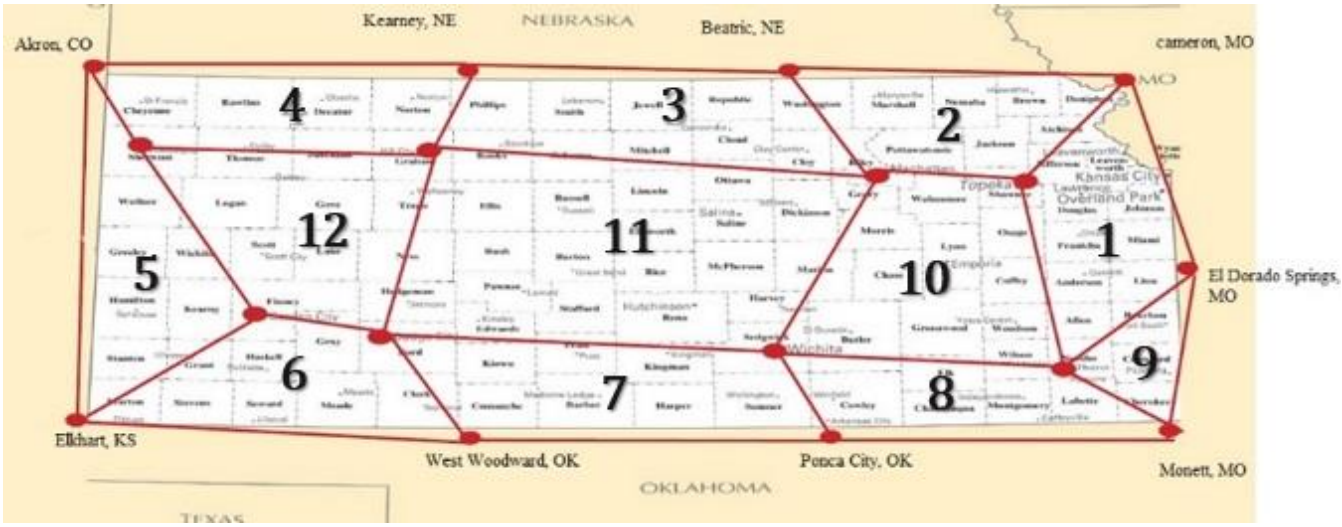

Figure 3.1: Kansas Interpolation Zones

Complete wind-speed records for the 45-year interpolation period were collected and extended for certain cities inside and around the Kansas borders, as represented by red dots in Figure 3.1. These cities represent the sampled locations that were used to interpolate county data throughout the study area. The complete records for these cities were used as base interpolation data to interpolate and build wind-time histories for all Kansas counties using finite element shape functions.

3.1 Raw and Extended Wind-Speed Data

Wind-time histories resulting from the developed wind model depend on the mean and high wind-speed records. However, because of gaps in the data collected from the National Weather Service and the 2020 weather forecast from WillyWeather

(https://www.willyweather.com/ks/riley-county/manhattan.html) for cities inside and around the Kansas borders, complete wind-speed data sets were repeated to reliably fill the gaps. The 45 years of data for each city was subdivided into nine groups, with each group consisting of five years of repeated data. For example, 1975–1979 was the first group of wind-speed data, and the first year of data, 1975, was repeated to represent the remaining four years in the group. The exact process was followed for the rest of the groups within the 45 years. One month was selected from each season, and its data was repeated for the other two months in the season throughout the entire year-groups.

3.2 County Spatial Wind-Speed Interpolation

As shown in Figure 3.1, this research discretized the state of Kansas into 12 geometrical interpolation zones (elements), with quadrilateral and triangular shapes. Two zones were triangular (Zone 5 and Zone 9), whereas the other zones were quadrilateral. Knowing the nodal high and medium wind-speed values at the corner of each zone allowed use of the finite element shape functions to approximate these specific wind speed quantities within the zone. Finite element shape functions interpolate the solution within the element using discrete values obtained at the mesh nodes.

The bilinear quadrilateral element, a two-dimensional finite element with natural and global coordinates, was used to model quadrilateral zones in the meshed Kansas map. This element is characterized by linear shape functions in the x and y directions. This is a generalization of the 4-node rectangular element. Each bilinear quadrilateral element has four nodes with two in-plane degrees of freedom at each node, as shown in Figure 3.2, with global coordinates of the four nodes denoted by (x_1, y_1), (x_2, y_2), (x_3, y_3), and (x_4, y_4). The node order for each element is essential—they must be listed in a counterclockwise direction starting from any node. The element was mapped to a square using the natural coordinates r and s, as shown in Figure 3.2, and the four shape functions for this element were listed as shown in Equation 3.1 in terms of the natural coordinates r and s (Kattan, 2003).

$$\begin{Bmatrix} N_1 = \frac{1}{4}(1-r)(1-s) \\ N_2 = \frac{1}{4}(1+r)(1-s) \\ N_3 = \frac{1}{4}(1+r)(1+s) \\ N_4 = \frac{1}{4}(1-r)(1+s) \end{Bmatrix}$$

Equation 3.1

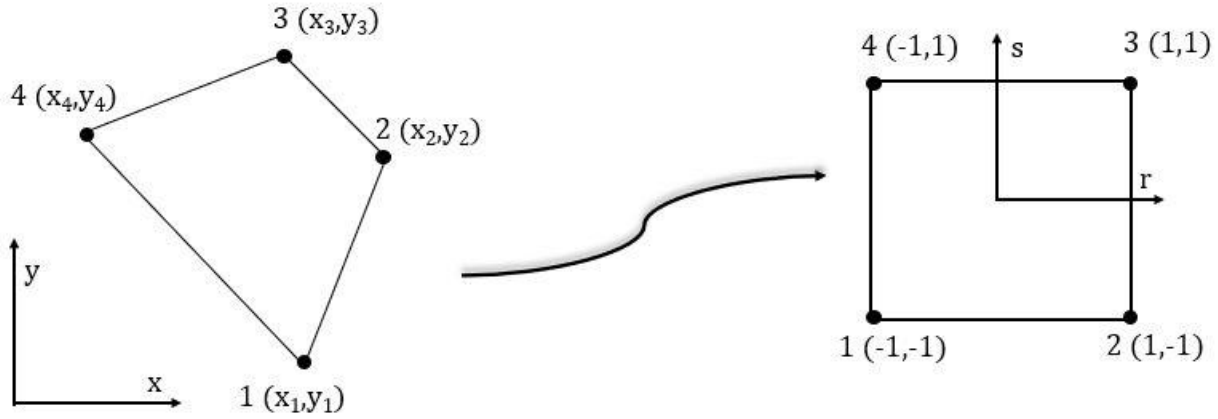

Figure 3.2: Mapping the Quadrilateral Element

Similarly, the linear triangular element, a two-dimensional finite element with natural and global coordinates, was used to model the triangular shapes. This element is characterized by linear shape functions. Each linear triangle has three nodes with two in-plane degrees of freedom at each node. The global coordinates of the three nodes are denoted by (x_1, y_1), (x_2, y_2), and (x_3, y_3). The element was mapped to a triangle using the natural coordinates *r* and *s*, as shown in Figure 3.3. Equation 3.2 details the three shape functions for this element.

$$\begin{Bmatrix} N_1 = \frac{1}{4}(1-r)(1-s) \\ N_2 = \frac{1}{4}(1+r)(1-s) \\ N_3 = \frac{1}{2}(1+s) \end{Bmatrix}$$

Equation 3.2

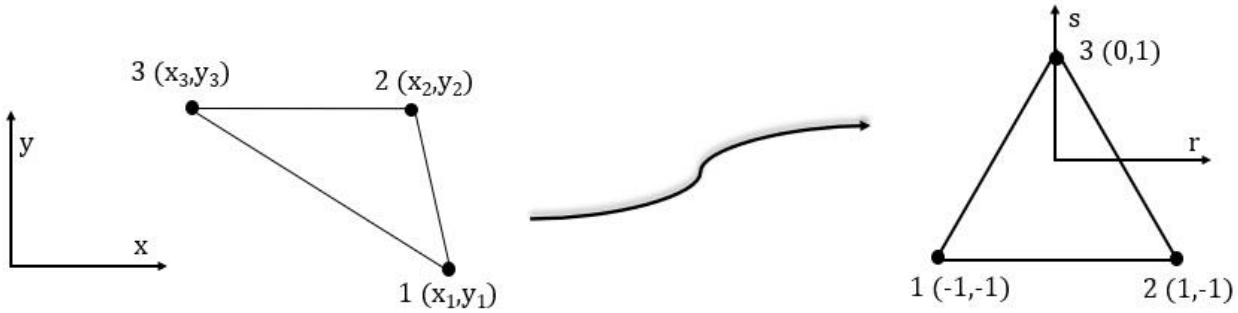

Figure 3.3: Mapping the Triangular Element

Complete wind speed records for 17 key cities were used to interpolate the county wind speeds. Coordinates for these cities were digitized along with counties' central locations (Table 3.1 and Table 3.2). Then, interpolation shape functions were recovered using the coordinates of the corner cities in each element along with the center location of the counties enclosed by that element, as shown in Figure 3.4.

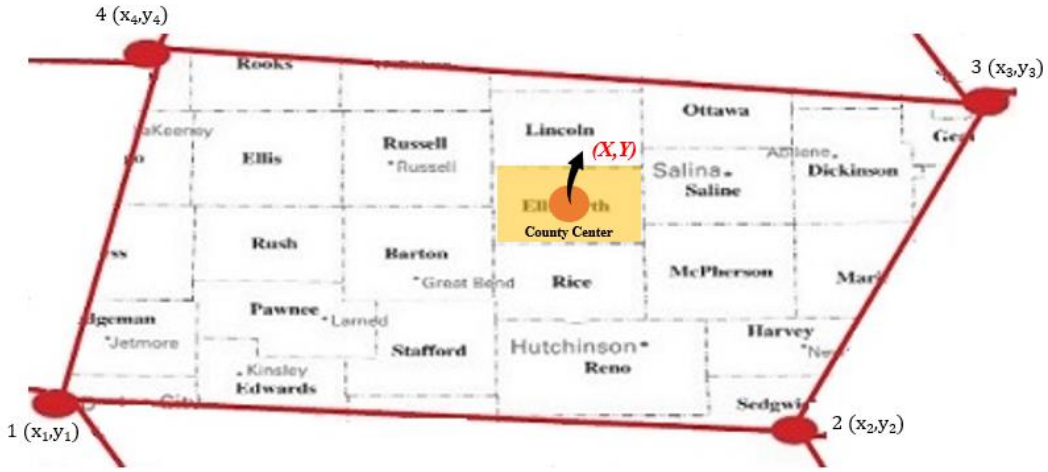

Figure 3.4: County Coordinates in Terms of City Coordinates

$$\{X\} = [X_i]\{N_i\} \qquad \textbf{Equation 3.3}$$

$$\mathbf{X} = N_1X_1 + N_2X_2 + N_3X_3 + N_4X_4 \qquad \textbf{Equation 3.4}$$

$$\mathbf{Y} = N_1Y_1 + N_2Y_2 + N_3Y_3 + N_4Y_4 \qquad \textbf{Equation 3.5}$$

$$\begin{Bmatrix} X \\ Y \end{Bmatrix} = \begin{bmatrix} X_1 & X_2 & X_3 & X_3 \\ Y_1 & Y_2 & Y_3 & Y_4 \end{bmatrix} \begin{Bmatrix} N_1 \\ N_2 \\ N_3 \\ N_4 \end{Bmatrix} \qquad \textbf{Equation 3.6}$$

Knowing the center coordinates X and Y and nodal cities' coordinates (x_1, y_1), (x_2, y_2), (x_3, y_3), and (x_4, y_4) allowed for the shape functions (N_1, N_2, N_3, N_4) to be calculated by solving the constraint optimization problem described below using Excel:

$$\text{Objective: } \mathrm{X} = N_1X_1 + N_2X_2 + N_3X_3 + N_4X_4$$

$$\text{Subjected to:}$$

$$\begin{cases} \mathbf{Y} = \boldsymbol{N_1Y_1 + N_2Y_2 + N_3Y_3 + N_4Y_4} \\ \boldsymbol{-1 \le r \le 1} \\ \boldsymbol{-1 \le s \le 1} \end{cases} \qquad \textbf{Equation 3.7}$$

Table 3.1: City Coordinates

City	X(Global)	Y(Global)
Akron	131.12	93.96
Kearney	442.608	98.64
Goodland	169.808	196.92
Hill City	409.872	204.72
Beatrice	729.736	108
Manhattan	803.144	245.28
Topeka	926.152	254.64
Cameron	1009.48	120.48
Elkhart	136.088	562.56
Garden City	283.896	425.28
Dodge City	387.064	451.8
West Woodward	461.464	584.4
Wichita	691.736	470.52
Ponca	738.36	582.84
Chanute	931.8	493.92
El Dorado Springs	1033.976	359.76
Monett	1021.08	573.48

Table 3.2: Coordinates of County Centers

County	x	y	County	x	y	County	x	y
Allen	958	430	Ellsworth	610	308	Lincoln	612	257
Anderson	958	379	Finney	300	401	Linn	1009	380
Atchison	949	176	Ford	408	461	Logan	263	274
Barber	551	530	Franklin	955	326	Lyon	853	345
Barton	549	341	Geary	782	264	McPherson	674	360
Bourbon	1007	433	Gove	340	273	Marion	742	362
Brown	920	133	Graham	412	210	Marshall	806	143
Butler	772	450	Grant	239	479	Meade	349	529
Chase	801	371	Gray	343	455	Miami	1009	327
Chautauqua	844	543	Greeley	176	341	Mitchell	610	204
Cherokee	1008	538	Greenwood	843	434	Montgomery	904	536
Cheyenne	188	141	Hamilton	177	412	Morris	792	313
Clark	414	530	Harper	624	538	Morton	175	534
Clay	731	210	Harvey	701	411	Nemaha	867	147
Cloud	674	192	Haskell	289	479	Neosho	956	481
Coffey	900	376	Hodgeman	405	401	Ness	405	341
Comanche	482	538	Jackson	894	197	Norton	408	143
Cowley	771	530	Jefferson	940	222	Osage	903	316
Crawford	1008	486	Jewell	611	142	Osborne	544	210
Decatur	346	142	Johnson	1009	275	Ottawa	675	246
Dickinson	735	285	Kearny	240	412	Pawnee	488	387
Doniphan	970	137	Kingman	620	483	Phillips	474	142
Douglas	955	276	Kiowa	485	483	Pottawatomie	827	204
Edwards	481	435	Labette	957	534	Pratt	548	472
Elk	843	495	Lane	343	339	Rawlins	268	140
Ellis	478	273	Leavenworth	986	224	Reno	623	423
Rice	611	364	Shawnee	898	252	Republic	672	136
Riley	777	214	Sheridan	346	211	Trego	415	273
Rooks	479	209	Sherman	185	208	Wabaunsee	848	264
Rush	480	335	Smith	542	141	Wallace	184	273
Russell	544	272	Stafford	553	410	Washington	741	141
Saline	674	360	Stanton	180	479	Wichita	228	339
Scott	289	340	Stevens	239	536	Wilson	904	479
Sedgwick	697	466	Sumner	699	531	Woodson	905	430
Seward	293	536	Thomas	275	208	Wyandotte	1019	237

After calculating the shape functions $\{N_i\}$, medium and high wind speeds were approximated using the nodal values for the element surrounding the county as follows:

$$\text{HWS} = N_1 * HWS_1 + N_2 * HWS_2 + N_3 * HWS_3 + N_4 * HWS_4$$

Equation 3.8

$$\text{MWS} = N_1 * MWS_1 + N_2 * MWS_2 + N_3 * MWS_3 + N_4 * MWS_4$$

Equation 3.9

3.3 Synthetic Wind-Time Histories

The spatial and temporal variation of wind velocity has two components: a daily mean component *U(z)* and daily fluctuating component *u (z, t)*, expressed through *U (z, t) = U(z)+u (z, t)*, where *U (z, t)* is the varying wind speed profile during the day (Cochran, 2012). A reference height (*z*) could be established for a specific structure, and the spatial dependency could be removed. Because wind is a random process with dynamic behavior that cannot be entirely predicted, the well-established Kaimal spectrum (Kaimal et al., 1972) was utilized to generate daily spectrum for the entire 45 years, using the following relationship:

$$S_K(f) = \frac{200 U_*^2 z}{U_z (1 + 50 \frac{fz}{U_z})^{5/3}}$$

Equation 3.10

Where:

S_K is the Kaimal spectrum,

z is the height above the ground (10 m (33 ft.)),

$U_*$is shear velocity,

U_z is the mean wind velocity at *z*, and

f is the specified frequency.

From Equation 3.11, the shear velocity is defined as:

$$U_* = \sqrt{\frac{\sigma_u^2}{6}}$$

Equation 3.11

Where the variance of the turbulent wind component is expressed as:

$$\sigma_u^2 = 6KU_z^2$$

Equation 3.12

The surface drag coefficient *K* (0.005) was valid for open terrain (Ginal, 2003).

Wind turbulence was simulated using weighted amplitude wave superposition by superimposing cosine waves over a frequency range of 3–300 Hz and randomly generated phase angles, as shown in Equation 3.13 (Iannuzzi & Spinelli, 1987):

$$u(t) = \sum_{i=1}^{N} \sqrt{2S_i f_i \Delta f}.\cos\left(2\pi f_i t + \emptyset_i\right)$$

Equation 3.13

Where:

$\emptyset_i$ is a randomly generated phase angle between 0 and 2π.

The resulting history yielded the following equation when it was combined with the mean daily wind speed:

$$U(t) = U_z + \sum_{i=1}^{N} \sqrt{2S_i f_i \Delta f}.\cos\left(2\pi f_i t + \emptyset_i\right)$$

Equation 3.14

After generating the turbulence spectrum, this fluctuating function combined with the mean wind speed on any given day to produce a complete wind-time history (Equation 3.14). Notably, however, the fully produced time history from Equation 3.14 is controlled by the mean speed and does not necessarily capture a specific high speed. To account for high wind speed on any given day, a scale-up factor (γ) was calculated as in Equation 3.15 and applied to Equation 3.14 for each day to make the maximum wind speed in the synthetic history equal the actual measured high speed for that day.

$$\gamma = \frac{(U_{max} - U_z)}{(U_{Kmax} - U_z)}$$

Equation 3.15

Where:

U_{max} is the actual maximum wind speed of the day,

U_z is the mean wind speed, and

U_{Kmax} is the maximum calculated wind speed in the synthetic time history for that day.

Then the new entire wind-time history was reproduced using Equation 3.16.

$$U(t) = U_z + \sum_{i=1}^{N} \gamma \sqrt{2 S_i f_i \Delta f} . \cos(2\pi f_i t + \emptyset_i)$$

Equation 3.16

Figure 3.5 shows a sample of generated wind-time histories for various mean wind speeds.

Each wind-speed value resulted from adding many cosine waves over the frequency content in addition to the mean value. However, this operation required massive calculations, even when using a high-speed computer if the frequency increment was too small. Time-history generation was performed on a 1-second scale each day, resulting in 86400 discrete speed values each day that had to be calculated to generate a history, while each speed was computed from imposing many cosine waves, which also required massive computations for building a 45-year database. Before proceeding with the thorough analysis, a sensitivity calculation was performed in which 798, 80, and 40 cosine waves were used to build synthetic wind speeds for the city of Wichita over a 45-year period to extract the number of wind cycles corresponding to each speed. The Rainflow method, explained in Section 3.5, was used to establish the distribution of speed versus the number of cycles for the three different numbers of cosine waves (Figure 3.6). As shown in the figure, the overall distribution was precisely identical, and the cycle variation followed a Gaussian distribution. Discretization using 80 waves was an excellent trade-off between computational speed and accuracy of results to generate the 45-year wind database. Table 3.3 summarizes the main parameters used in the final wind-speed simulation.

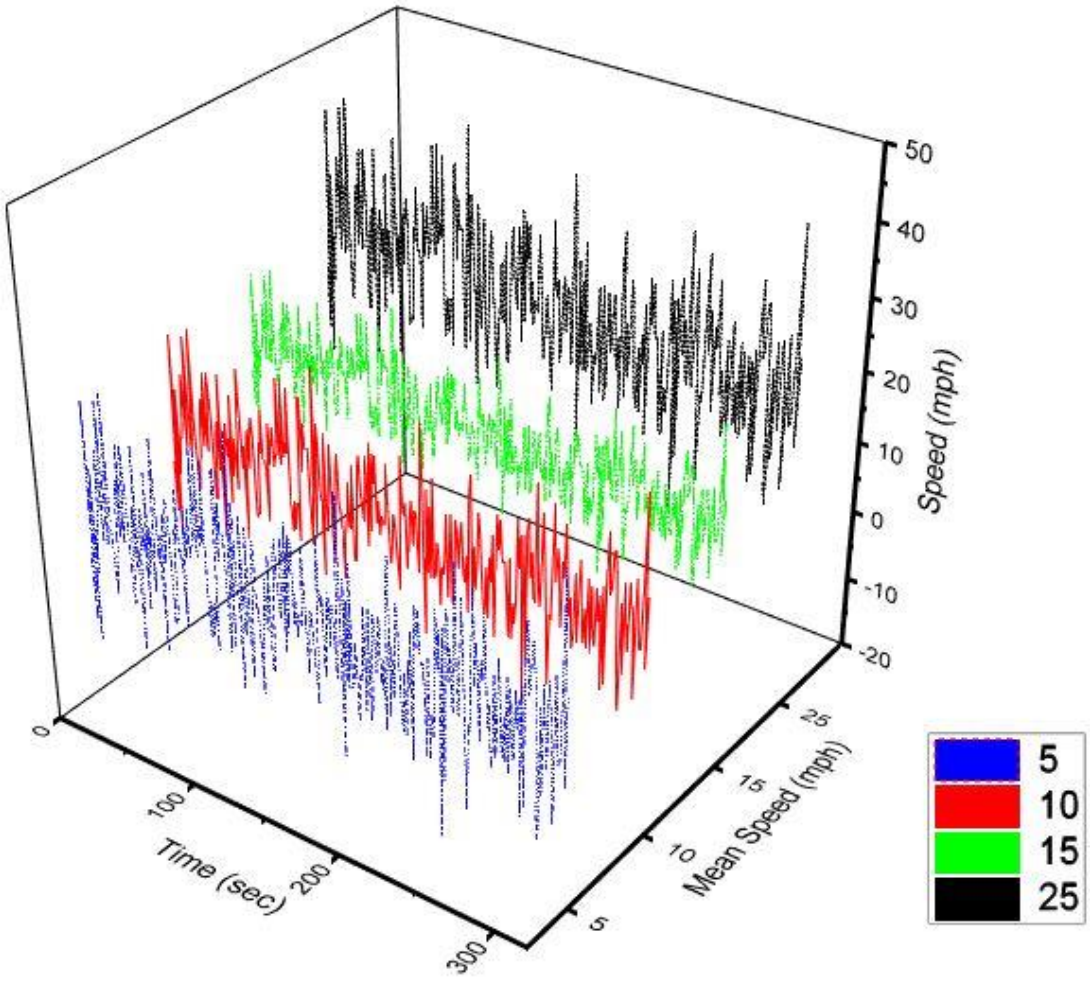

Figure 3.5: Wind-Time Histories for Various Mean Wind Speeds

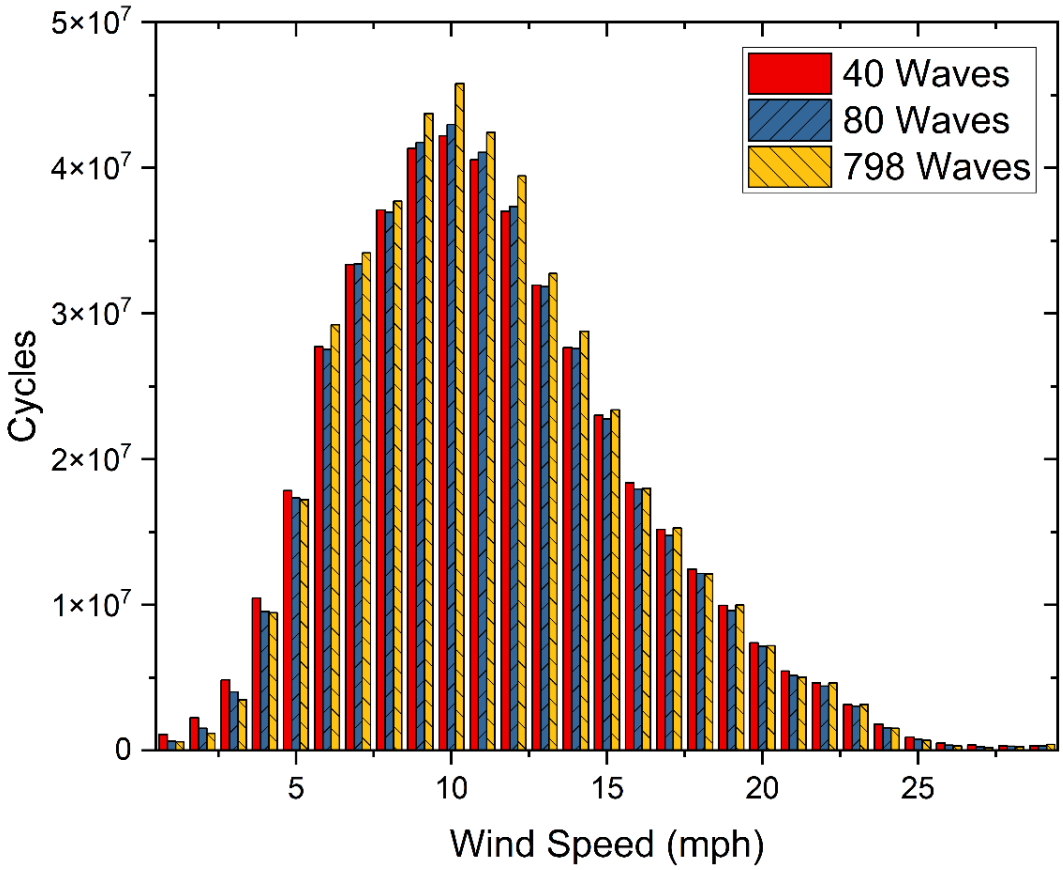

Figure 3.6: Speed vs. Number of Cycles for 45 Years in Wichita for Cosine Waves

Table 3.3: Main parameters in Wind-Speed Simulation

Parameter	Value
Surface roughness class	Open terrain (k = 0.005)
Height above ground	33 ft
U_z	Vary
U_{max}	Vary
Fluctuation wind speed spectrum	Kaimal
Length of time history	One day
Timestep	1 s
Frequency range	3–300 Hz
Number of cosine waves in superposition	80

3.4 Validation of Synthetic Time History

The wind model established, in this study, was validated against a real wind-speed profile obtained for the city of Manhattan from the National Oceanic and Atmospheric Administration (NOAA) through WillyWeather (https://www.willyweather.com/ks/riley-county/manhattan.html). The

average wind speed for September 23, 2020, was 7 mph, and the highest wind speed was 13.8 mph. The wind profile was built by inputting these parameters into the proposed wind model to validate the fluctuation behavior, as shown in Figure 3.7. Time history was plotted by selecting wind-speed values that corresponded to the time step depicted in the actual wind-time profile. As shown in the figure, simulated wind histories accurately reflected the characteristics of actual measured, natural wind records. These simulations produced a wind-time profile that adhered closely to the fluctuations of the natural wind time history. Overall, simulated wind histories accurately represent actual in-service wind loading conditions experienced by civil structures.

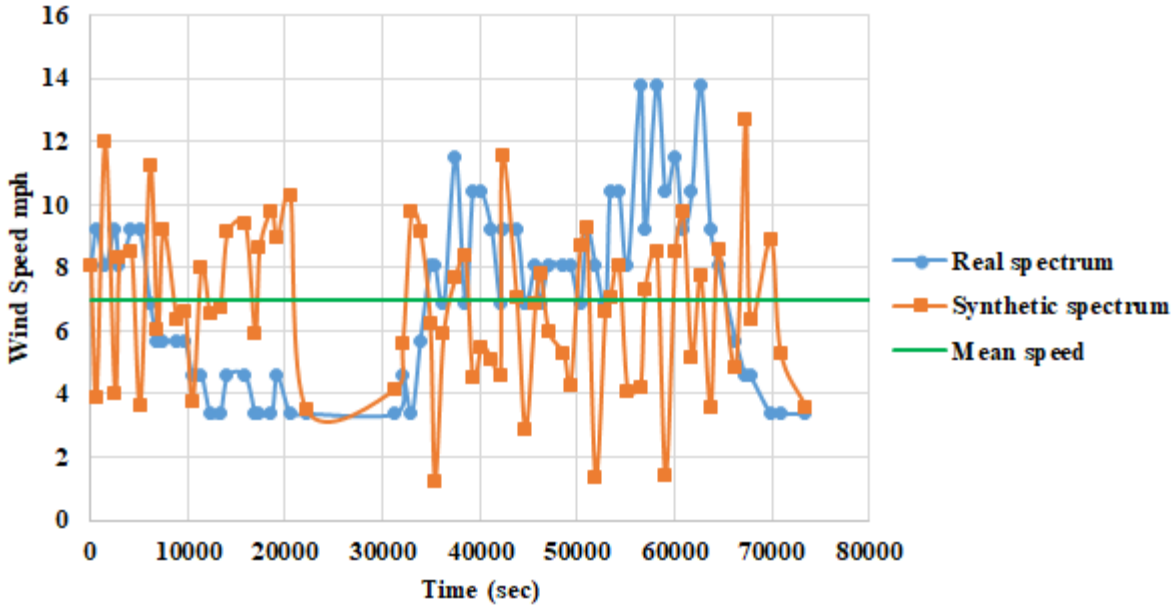

Figure 3.7: Real and Synthetic Wind Profiles for Mean 7 mph and High 13.8 mph (1 mph = 1.609 km/h)

After validating the resulting time histories and selecting the appropriate modeling parameters (Table 3.3), the procedures shown in Figure 3.8 were implemented in C# code to produce a 45-year database of wind-time histories and daily synthetic wind profiles for all counties in Kansas. Figure 3.9 shows the database for any county in Kansas stored in a matrix form. After generating the database, the Rainflow counting technique was implemented to convert the irregular wind-time histories into a usable number of constant amplitude cycles.

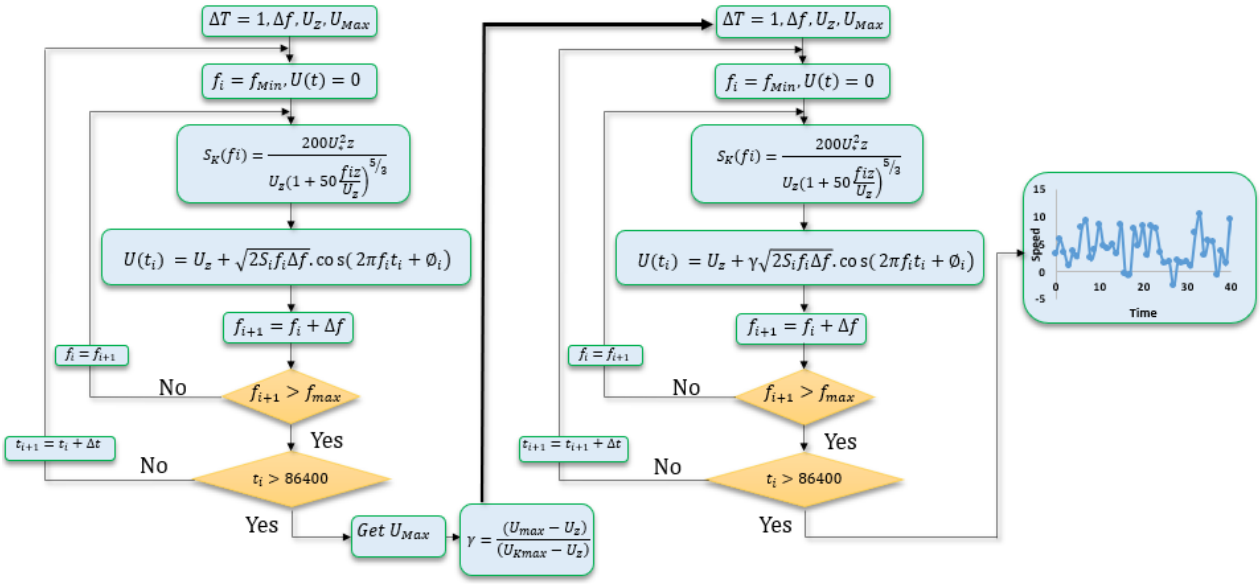

Figure 3.8: Flowchart for Wind-Time Histories

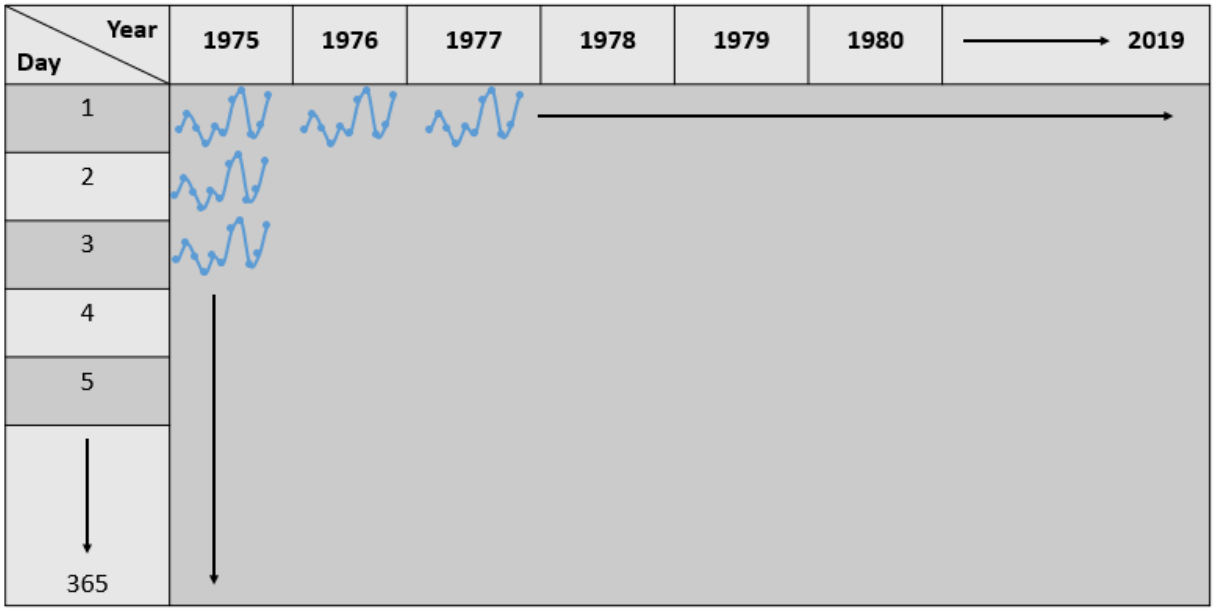

Figure 3.9: Wind-Time History Databases for Any Kansas County

3.5 Rainflow Counting Technique

The wind-time histories generated for the 45 years of data represented highly irregular variations of speed with time. To identify how each wind speed cycle was extracted, the Rainflow counting technique, developed by Matsuishi and Endo (1968), was adapted to convert the irregular time histories to cycles. The approach identified closed hysteresis loops in a non-periodic stress

response. The title of the technique, Rainflow counting, came from the idea that when turned sideways, the response versus time looks like a Chinese pagoda, and the stress cycles can be envisioned as raindrops falling from the pagoda. The algorithm was borrowed from ASTM E1049 (2017) and implemented into a computer code to extract the cycle database for 45 years. Figure 3.10 demonstrates the Rainflow counting technique.

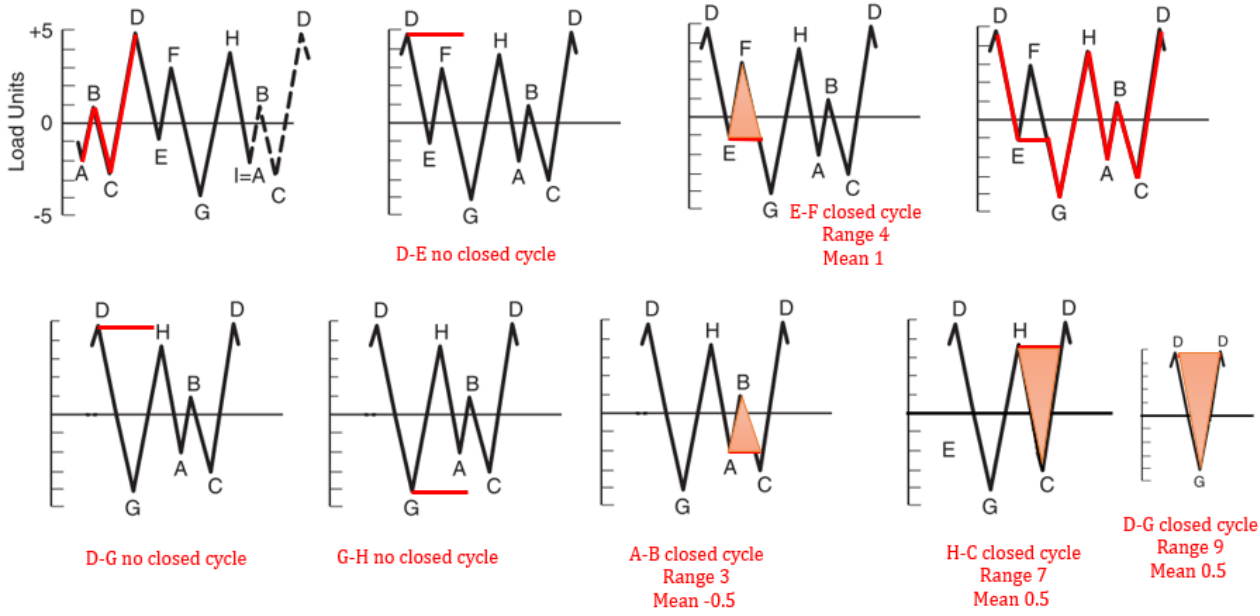

Figure 3.10: Rainflow Counting Example

Implementing the Rainflow counting technique for each daily wind-time history resulted in a speed-cycle matrix that represented the number of cycles for each wind speed in a day, obtained from grouping the cycles in 0.5 range scale. Figure 3.11 shows the speed-cycle matrix.

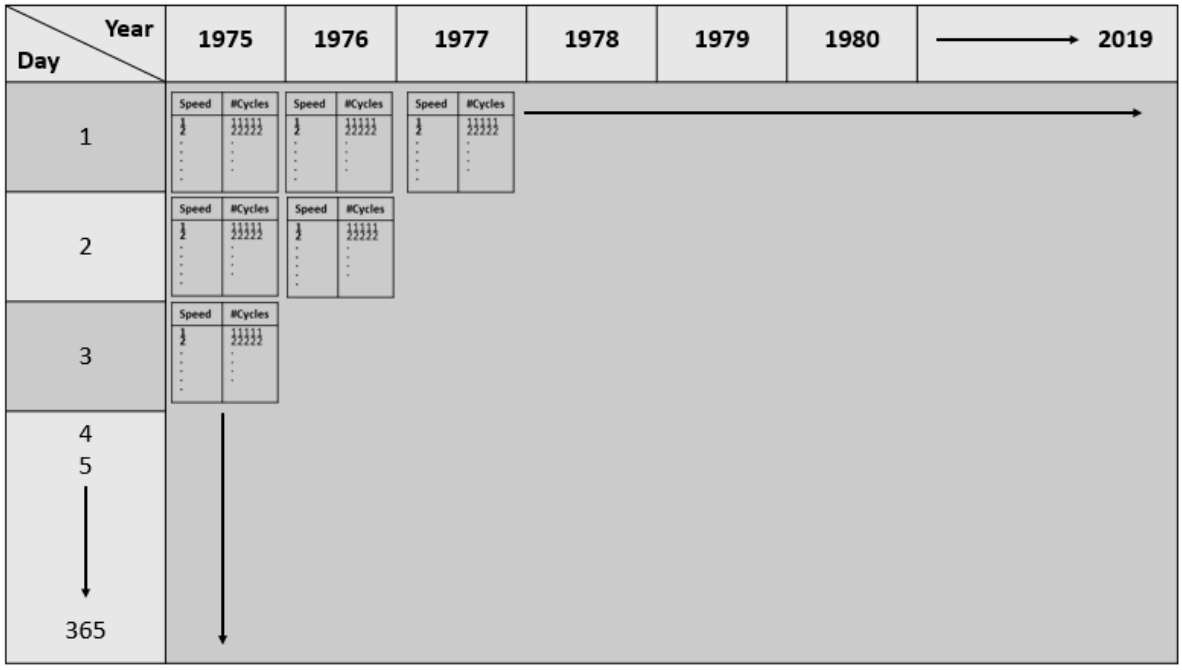

Figure 3.11: Speed-Cycle Matrix

Chapter 4: Software Development

The proposed procedures require massive calculations prior to producing the wind-cycle profile for any given county. A database for all counties and cities was generated for 1975–2019 and stored in a matrix format to effectively produce any county profile for any given period. Then a user-friendly interpolation software was built to compute the complete wind-cycle profile for any given county in any time range. Cycles Generation software is an object-oriented program written in C# language to efficiently generate wind-cycle profiles from a previously developed database. This software requires Microsoft Excel to be installed on the working machine since the generation process requires access to an Excel file that contains all the background data. Moreover, the software can present a graph showing the wind-cycle distribution and text file as an external file. The software interface contains two parts: the input part provides the required information for any county or city, and the output part displays the results for the county or the city.

4.1 Input Interface

The software input screen was divided into one section that displayed the Kansas state map and another section with the time selection section to specify the starting and ending interpolation date. Figure 4.1 shows the software input interface. The core cities shown in brown on the Kansas map are the cities that use the actual measured wind speeds, while the counties shown in black represent the interpolated counties. The speed-cycle profiles for a county were quickly produced by clicking on the desired county in the map and selecting the starting date from the “Year Built” box and the end date from the “Inspection Year” box. The software then grouped all the wind speed-cycles in that given time span and displayed them on the results screen. The inspection year must be greater than the year built, otherwise the software displays an error message. The interpolation date began in 1975 and ran until the year 2035, while the inspection years ran from 2010 to 2064. The most extended period the software can handle is 1975–2064.

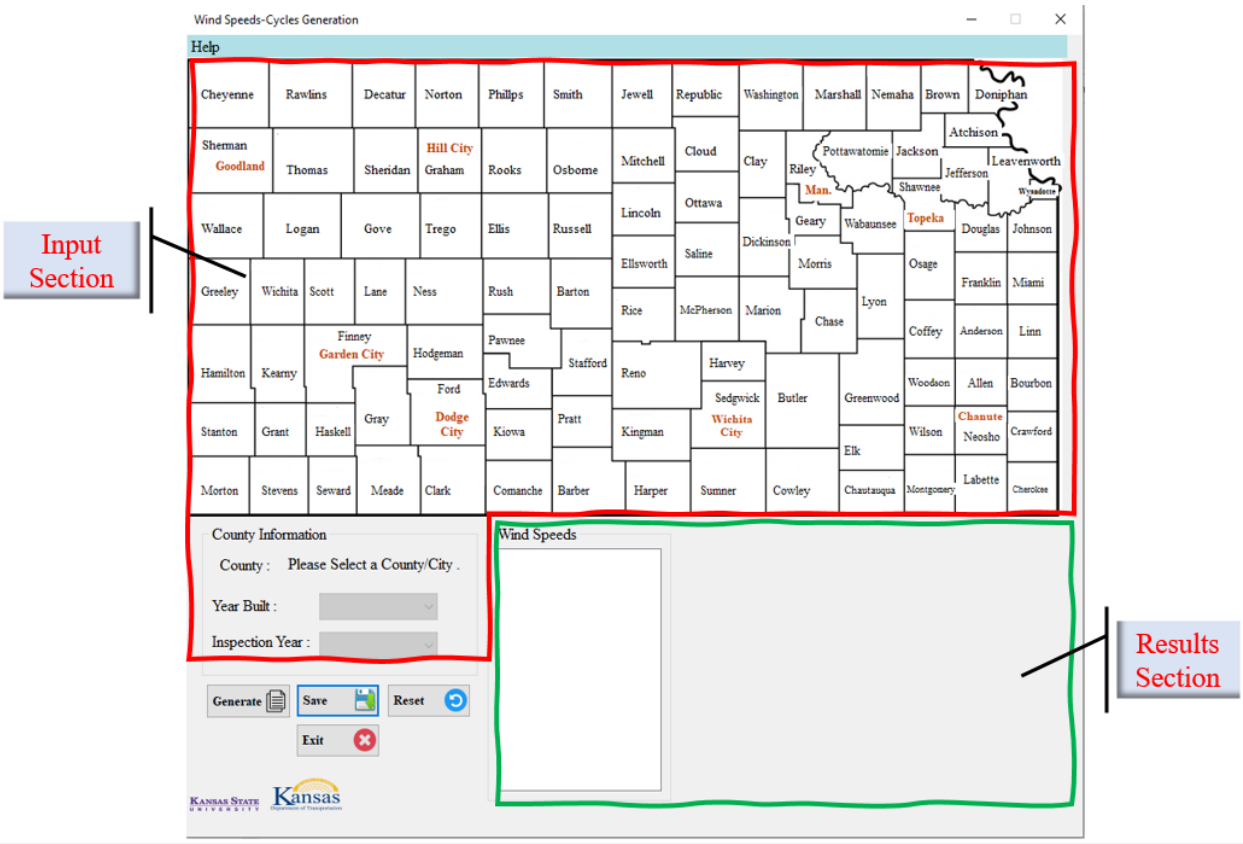

Figure 4.1: Speed-Cycle Generation Input Interface

4.2 Results

After specifying the input data, clicking the “Generate” button from the control box produced speed-cycle data based on the given information. The results were shown as a list in a white box and a histogram representation, as shown in Figure 4.2. The user could then save the results in a separate file on the hard disk, and the output file was formatted to be used in other software, such as the cantilever and butterfly fatigue simulators. Figure 4.3 shows the saving screen and sample output file. This software generated the results for the period 1975–2019 and extrapolated the results for the time interval 2020–2064 by mirroring the data from the end of December 2019 to the beginning of the January 2020 timeline. Figure 4.4 demonstrates the mirroring technique.

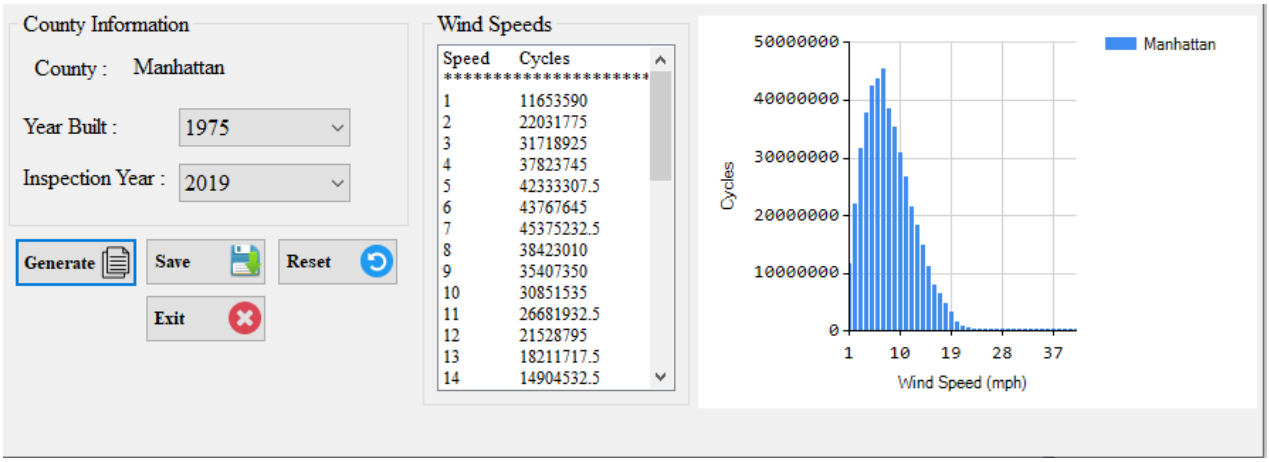

Figure 4.2: Results Screen

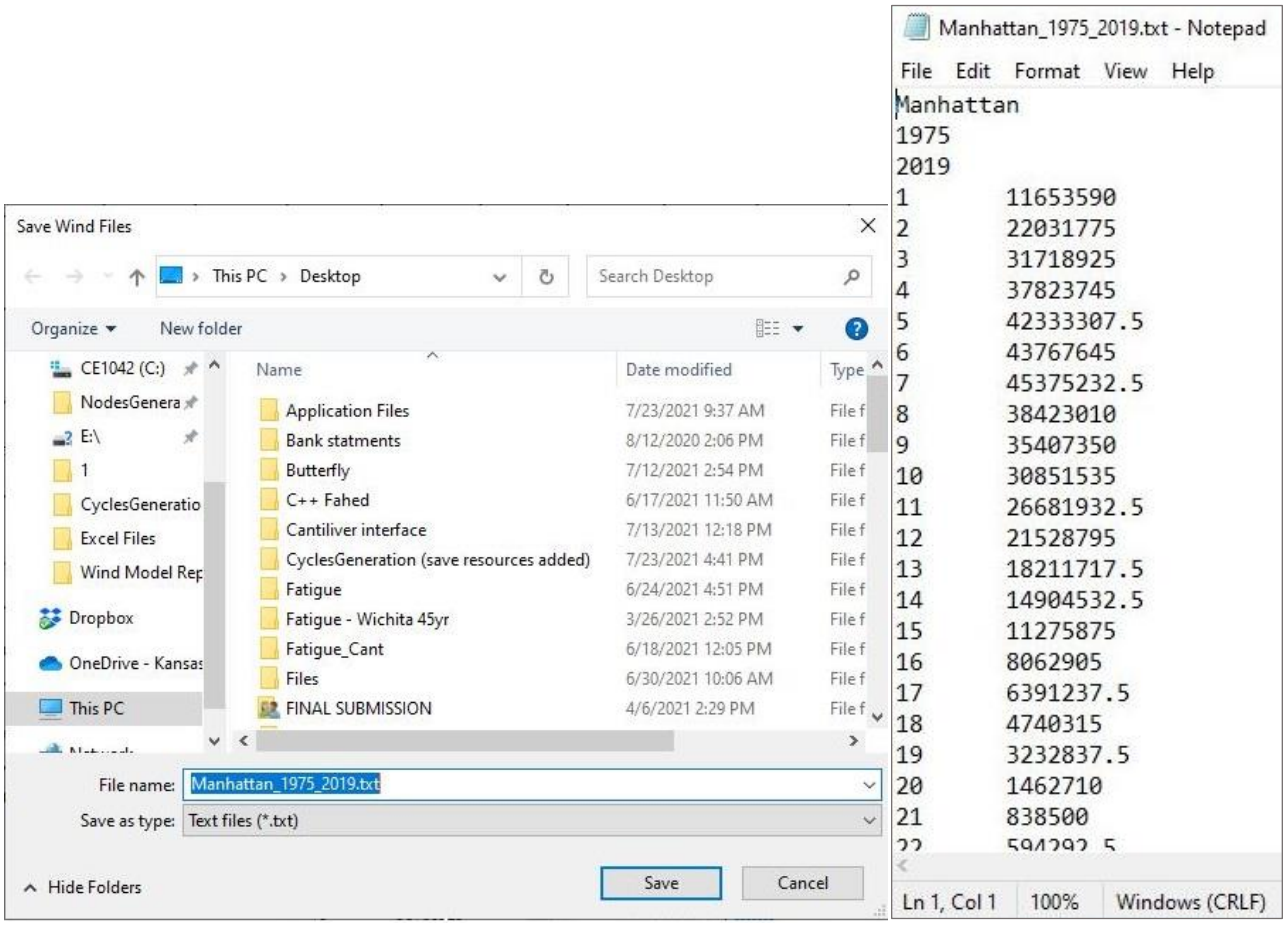

(a) (b)

Figure 4.3: (a) Save Box Screen; (b) Sample File

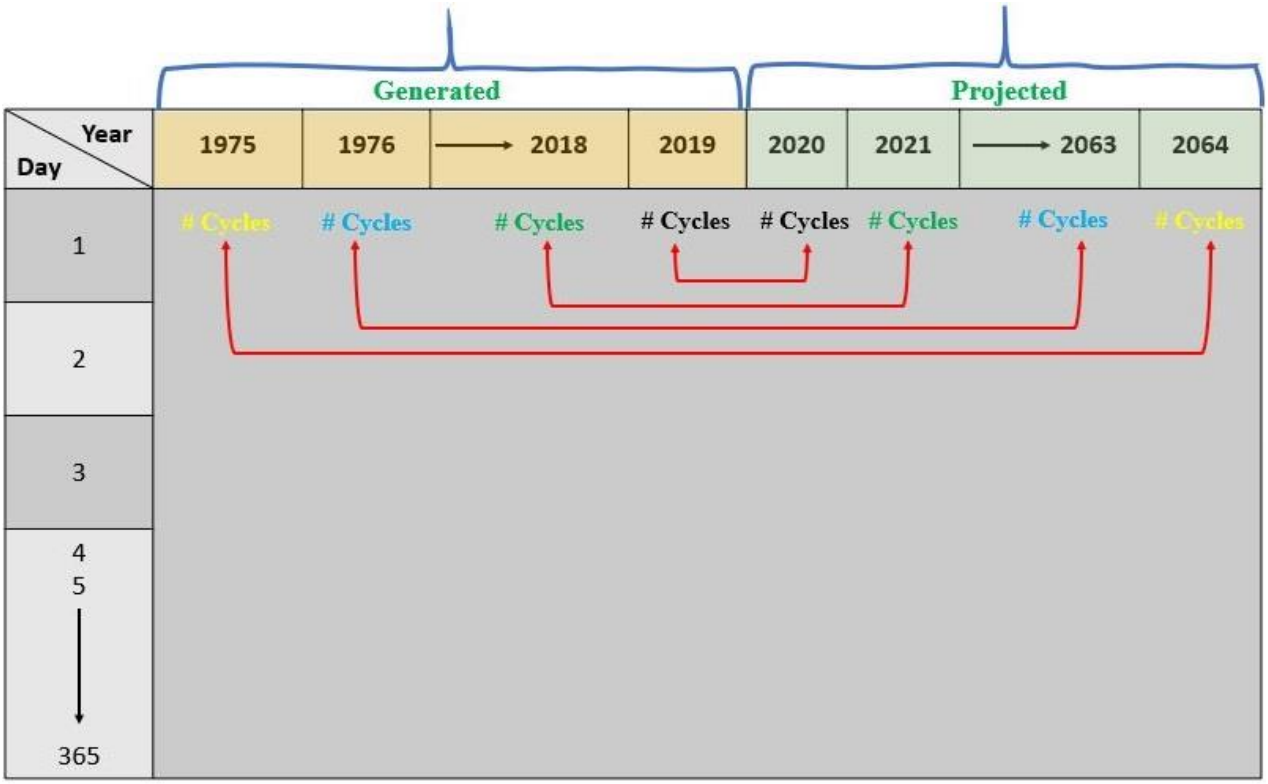

Figure 4.4: Database Mirroring

Chapter 5: Results and Discussion

This section provides wind speed records for counties and cities in Kansas and compares the resulting wind cycles for Wichita with its counterpart resulting from the deterministic wind model developed by Alshareef et al. (2019). For example, as shown in Figure 5.1, Zone 8 is a quadrilateral element consisting of four nodal cities: Ponca City, Oklahoma; Monett, Missouri; Chanute, Kansas; and Wichita, Kansas. Based on the developed approach, interpolation of the wind-speed data for Cowley County assumed that significant data contribution would come from Wichita and Ponca City since they are closest to the center of Cowley County. To calculate each city's weight function, global coordinates were obtained for the four cities and the county's center, as shown in Table 5.1.

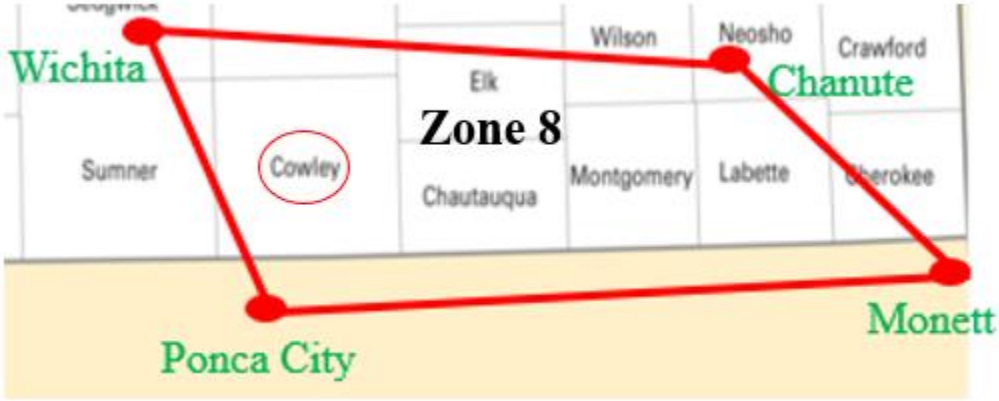

Figure 5.1: Zone 8

Table 5.1: Zone 8 Coordinates

City	X	Y
Wichita	691.736	470.52
Chanute	931.8	493.92
Ponca City	738.36	582.84
Monett	1021.08	573.48
Cowley	771	530

The weight functions were obtained by solving Equation 3.7, resulting in {N1 = 0.40864, N2 = 0.108845, N3 = 0.10149, N4 = 0.381025}, which correspond to city contributions (Ponca City, Monett, Chanute, and Wichita, respectively). For any given day, the county's medium or high wind speed equaled the city's weight function multiplied by the corresponding wind speed for that city. Figure 5.2 shows the high and medium wind-speed variations for the cities surrounding Zone 8 for four key months in 1975. The red line graph represents the variation in wind speed for interpolated Cowley County. The overall trend of the derived data followed the cities' trend, and the values represent the weighted average values.

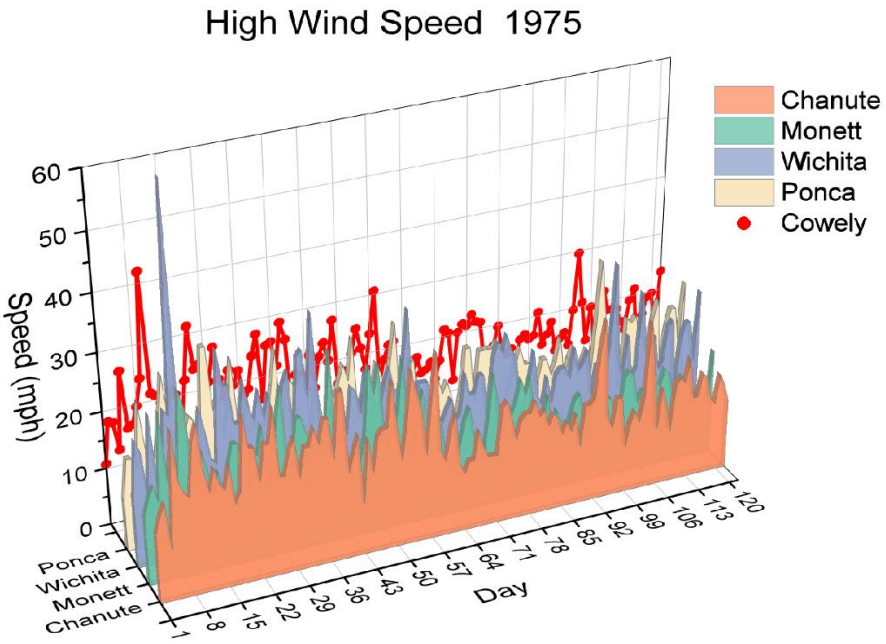

(a)

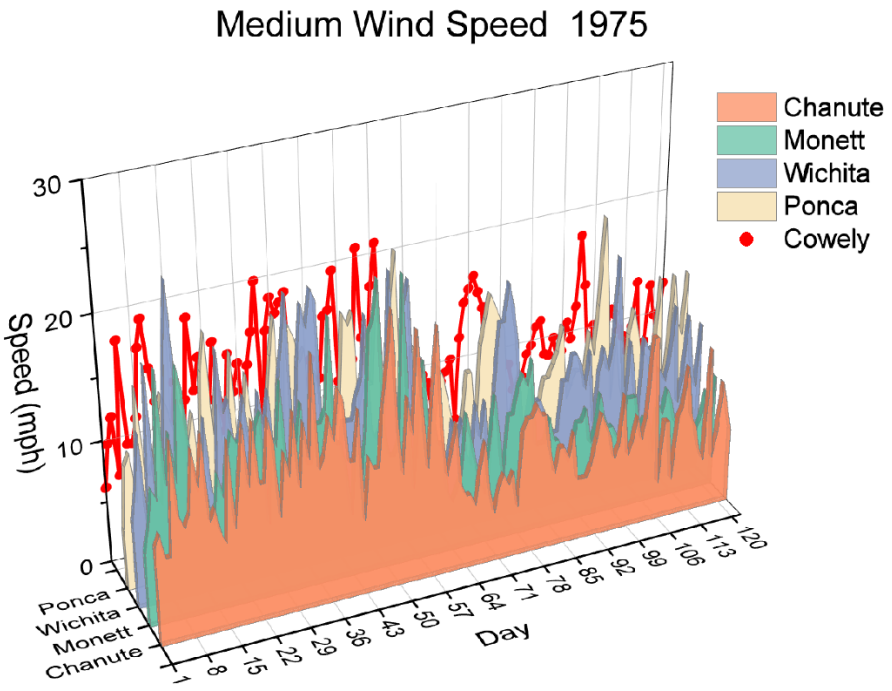

(b)

Figure 5.2: (a) High Wind Speeds for Zone 8; (b) Medium Wind Speeds for Zone 8

5.1 Comparison with Deterministic Model

The wind fluctuation model developed by Alshareef et al. (2019) simulated the variation in wind speed over time, assuming equal distances between high and medium speeds and between medium and low speeds to overcome missing wind-speed records for the low values. After preparing all the wind-speed records, this study assumed a quarter-day recurring model to quantify the number of wind-speed cycles, assuming a full sinusoidal cycle of high, medium, and low wind-speed fluctuations. In addition, the model assumed that high wind speed dominated one-quarter of the day, while medium wind-speed cycles dominated half the day, meaning the low wind-speed cycle controlled the remaining quarter of the day. This model is called the deterministic model because the wind-cycle fluctuation is predetermined. Consequently, wind-speed distribution throughout the day was specified as follows:

- 1 hour = 3600 seconds
- 1 day = 24 hours
- 1 day = 3600 x 24 = 86400 seconds
- High Speed = 86400 x 1/4 = 21600 seconds/day
- Medium Speed = 86400 x 2/4 = 43200 seconds/day
- Low Speed = 86400 x 1/4 = 21600 seconds/day

To build the number of cycles for a city, the number of occurrences for each high, medium, and low wind speed must be determined, assuming a constant 1 Hz frequency for each cycle. Then the number of cycles can be calculated based on the quarter-day recurring model. Table 5.2 classifies wind speeds in January for 1975–1979 for Wichita. Table 5.3 was established, and the number of cycles was found using Equation 5.1 and Equation 5.2.

$$\textbf{Total count based on ¼ model} = \#\boldsymbol{of\ high\ speeds} \times \frac{1}{4} + \#\ \boldsymbol{of\ medium\ speeds} \times \frac{1}{2} + \#\ \boldsymbol{of\ low\ speeds} \times \frac{1}{4}$$

Equation 5.1

$$\textbf{Total cycles} = \textbf{Total count based on ¼ model} \times \textbf{86400}$$

Equation 5.2

Table 5.2: Estimated Wind Speeds for January (Wichita)

Years - 1975, 1976, 1977, 1978, 1979							
Day	**High**	**Medium**	**Low**	**Day**	**High**	**Medium**	**Low**
1	12	7	2	17	16	8	0
2	22	10	0	18	15	7	0
3	20	14	8	19	34	19	4
4	12	6	0	20	28	14	0
5	26	19	12	21	28	15	2
6	14	9	4	22	21	11	1
7	14	8	2	23	21	12	3
8	26	13	0	24	28	15	2
9	25	20	15	25	23	11	0
10	63	25	0	26	21	9	0
11	23	16	9	27	26	15	4
12	21	14	7	28	21	12	3
13	18	9	0	29	25	15	5
14	17	8	0	30	20	9	0
15	25	7	0	31	20	15	10
16	21	14	7				

Table 5.3: Number of Cycles for January (Wichita)

Years - 1975, 1976, 1977, 1978, 1979					
Speed	**# of High Speeds**	**# of Medium Speeds**	**# of Low Speeds**	**Count Based on Quarter-Day Model**	**Total Cycles**
0	0	0	65	16.25	1404000
1	0	0	5	1.25	108000
2	0	0	20	5	432000
3	0	0	10	2.5	216000
4	0	0	15	3.75	324000
5	0	0	5	1.25	108000
6	0	5	0	2.5	216000
7	0	15	10	10	864000
8	0	15	5	8.75	756000
9	0	20	5	11.25	972000
10	0	5	5	3.75	324000
11	0	10	0	5	432000
12	10	10	5	8.75	756000
13	0	5	0	2.5	216000
14	10	20	0	12.5	1080000
15	5	25	5	15	1296000
16	5	5	0	3.75	324000
17	5	0	0	1.25	108000
18	5	0	0	1.25	108000
19	0	10	0	5	432000
20	15	5	0	6.25	540000
21	30	0	0	7.5	648000
22	5	0	0	1.25	108000
23	10	0	0	2.5	216000
25	15	5	0	6.25	540000
26	15	0	0	3.75	324000
28	15	0	0	3.75	324000
34	5	0	0	1.25	108000
63	5	0	0	1.25	108000

Figure 5.3 compares wind speeds and number of cycles for both models for January 1975–1979.

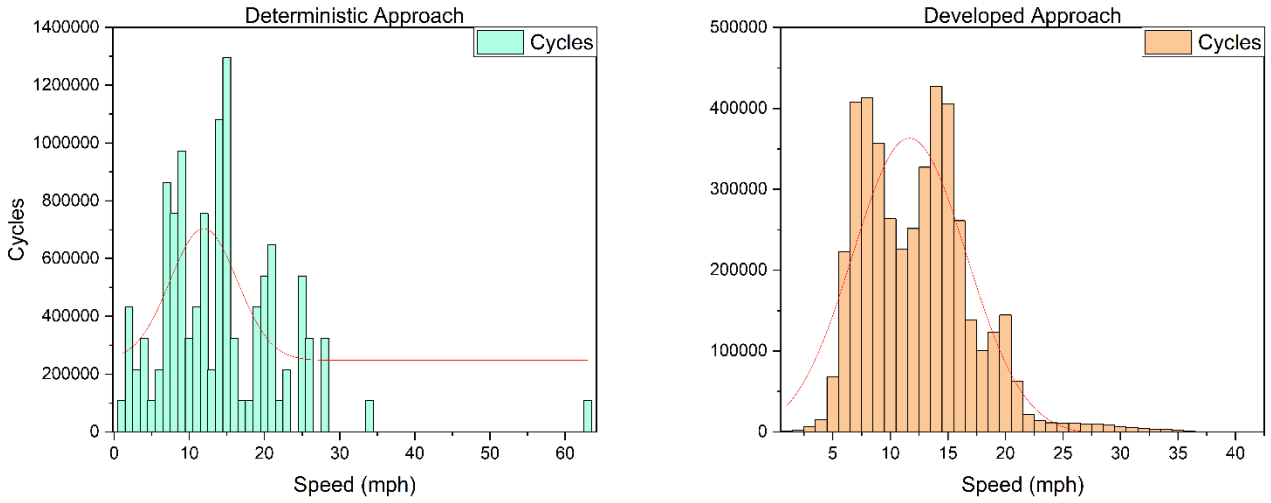

(a) (b)

Figure 5.3: Speed vs. Cycles: (a) Deterministic Approach; (b) Developed Approach

Figure 5.4 compares total cycles of both approaches over the entire 45-year study period for the city of Wichita. As shown, the number of cycles from the deterministic approach is higher than the developed approach for all wind speeds due to the primary assumption of the deterministic approach that is based on a 1 Hz fluctuation model. However, the developed approach assumed harmonic excitations in a range of 3–300 Hz, and the derived time histories resulted from superimposing 80 incremental cosine waves. Although both curves follow a Gaussian distribution to a good extent, the developed approach shows a higher R^2 (0.9767) than the deterministic approach (R^2 = 0.9469).

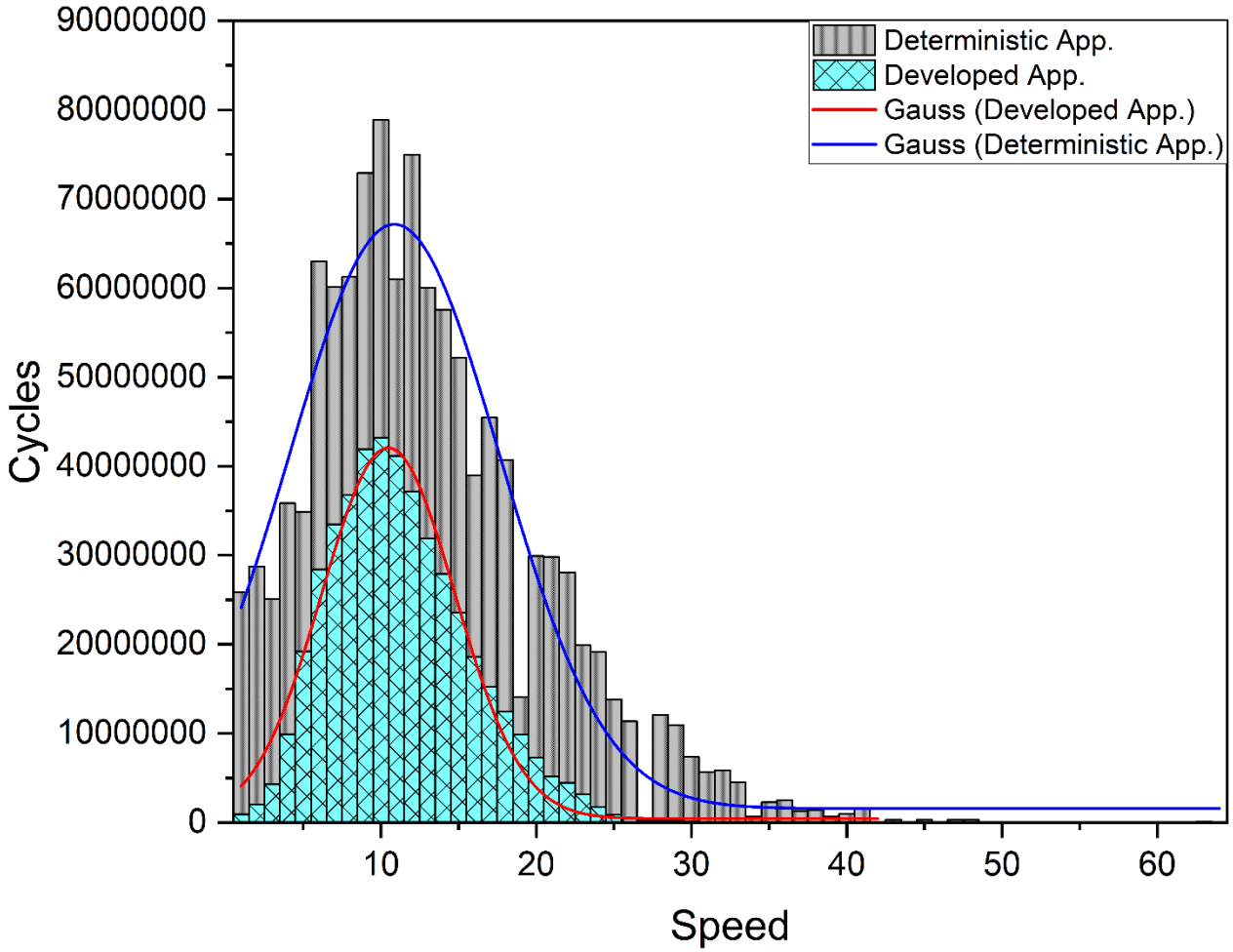

Figure 5.4: 45-year Cycles for Both Approaches for Wichita

Chapter 6: Interpolation Assessment

The finite element interpolation technique interpolates records for unsampled locations from records of sampled locations based on the average contribution for each city in the meshed study area. Method accuracy depends on mesh size—a smaller mesh results in more accurate, reliable results because the spatial dependency of the interpolated phenomena is minimal. On the other hand, larger areas result in deviation from the interpolated data from the actual measurements. In the absence of actual data, the Kansas map was re-meshed, as shown in Figure 6.1, to form two new zones to recover wind records for the city of Wichita. Wind-speed records from the four nodal cities bounding each zone were interpolated and compared to the actual measured values, and the high and mean wind speeds were evaluated for four months for all the year groups to statistically evaluate the results reliability of the developed method.

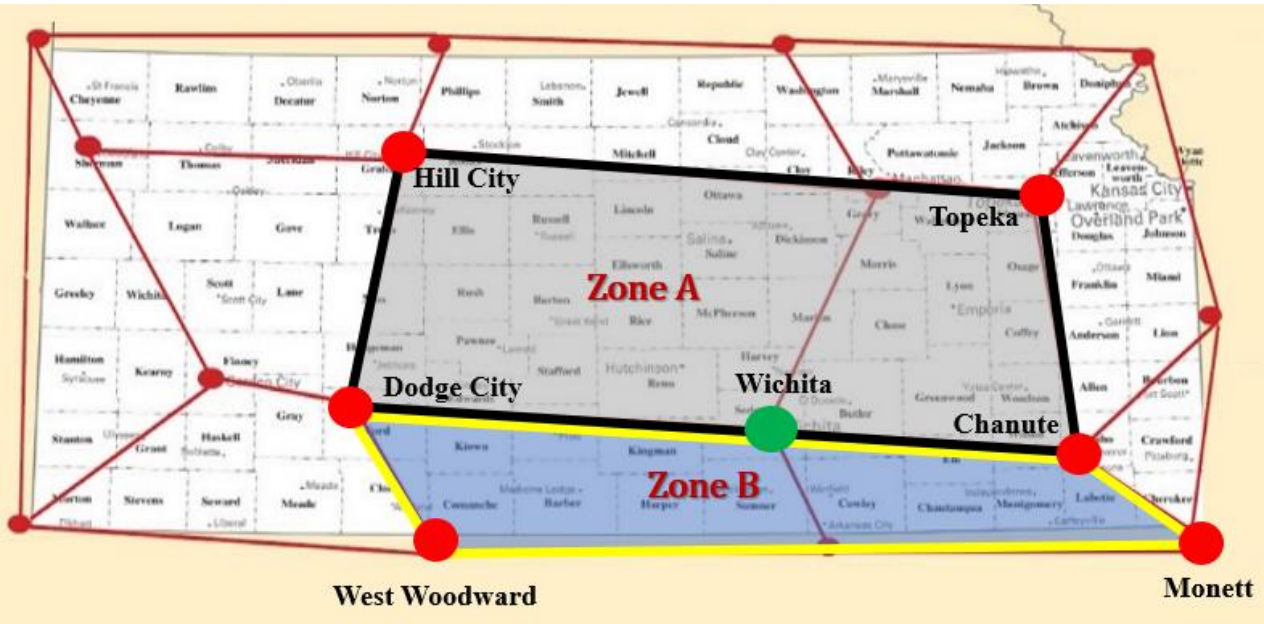

Figure 6.1: New Interpolation Zones (Zone A and Zone B)

Accurate interpolation zone selection is essential to achieve accurate results. Zones should be selected as closely as possible to the interpolated city since measured values closest to the prediction location have more influence on predicted values than values far from the prediction location. Figure 6.2 and Figure 6.3 show the correlation between predicted high and mean wind

speeds in Zone A and Zone B, respectively, for the years 1975–2019. As shown in the plots, values for the high and mean daily wind speeds are identical regardless of the zone used in the interpolation. Because the shape function values differ in both cases to account for the distance between the interpolated cities and the city of Wichita, their agreement along the 45° line testify to the reliability of the formulated interpolation.

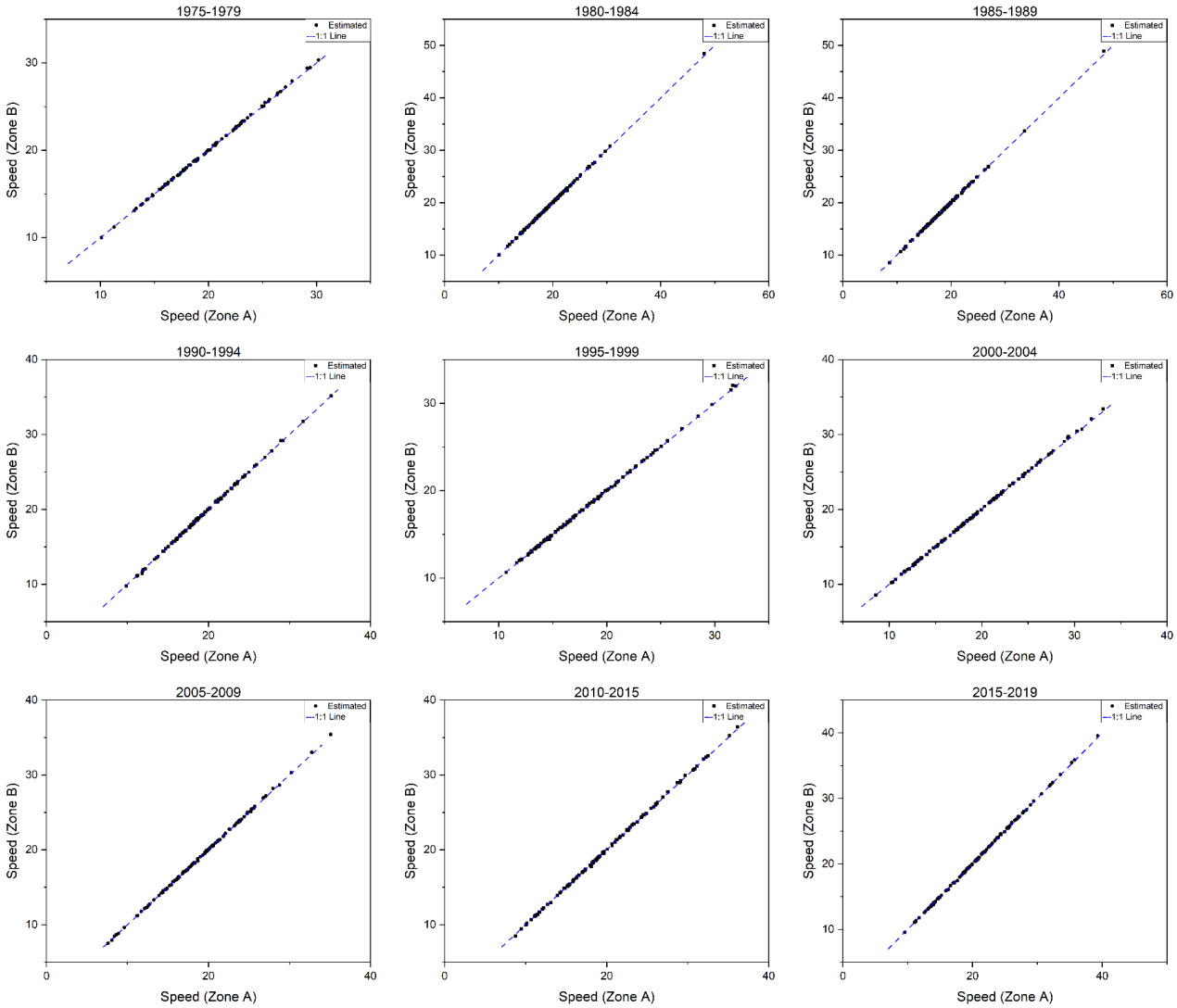

Figure 6.2: Predicted Daily High Wind Speeds for Zone A and Zone B in Wichita, 1975–2019

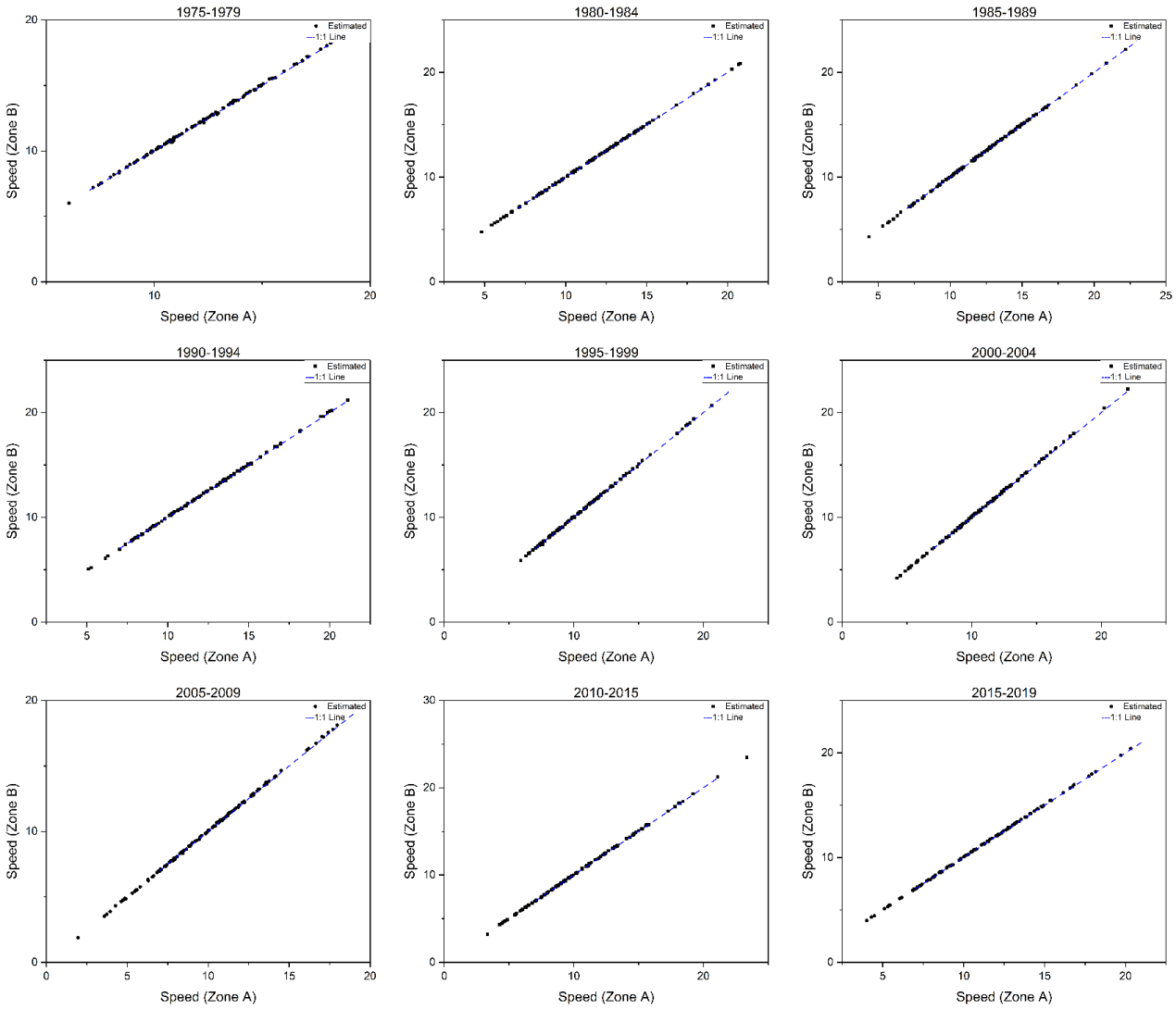

Figure 6.3: Predicted Daily Mean Wind Speeds for Zone A and Zone B in Wichita, 1975–2019

Since Zone A and Zone B displayed the same results, the predicted values obtained from Zone A were compared to the actual measured values. Figure 6.4 and Figure 6.5 present the measured and predicted high and mean wind-speed values, respectively, for 120 days in Wichita.

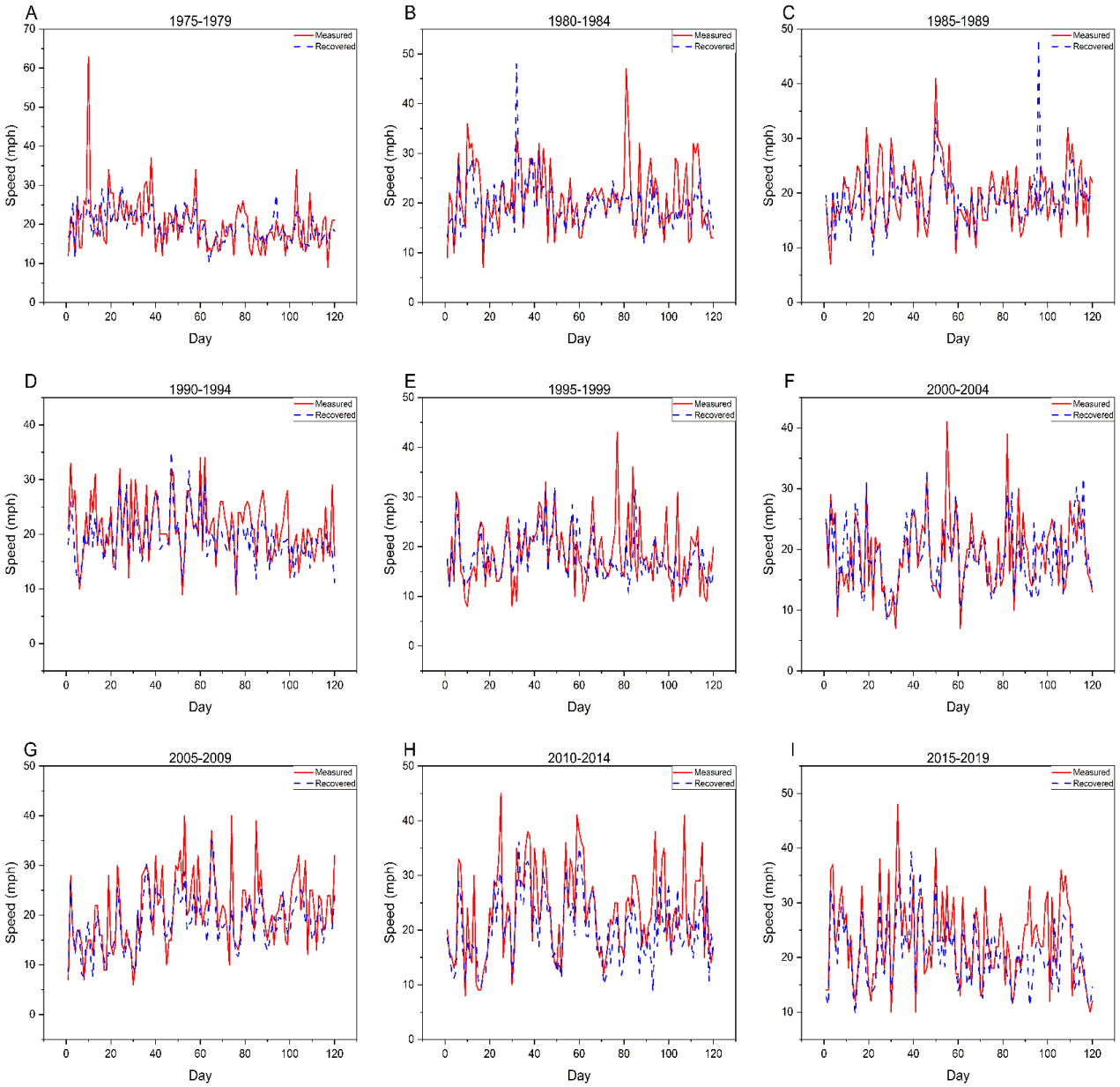

Figure 6.4: Measured vs. Predicted High Wind Speeds in Wichita for 120 Days

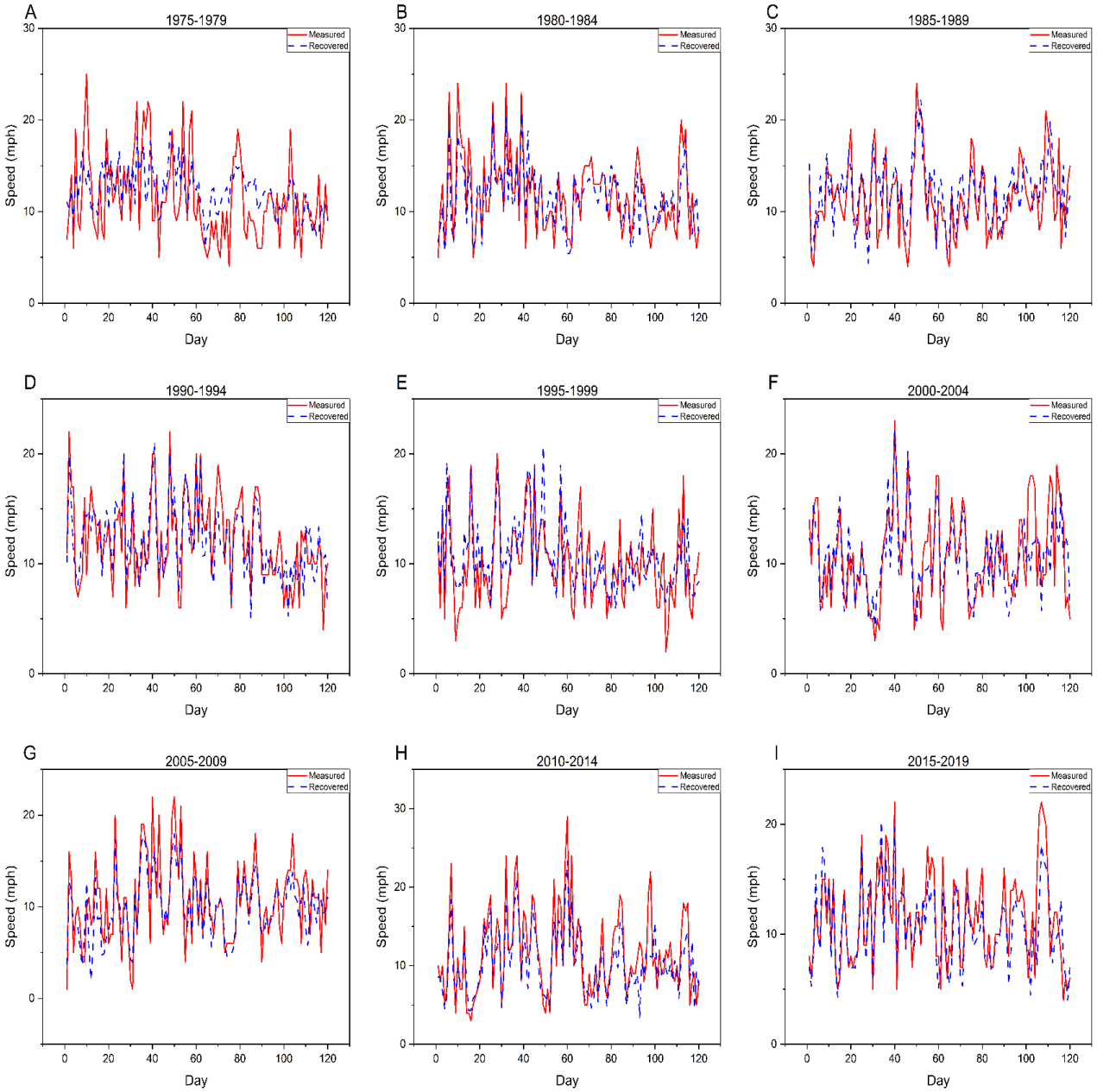

Figure 6.5: Measured vs. Predicted Mean Wind Speeds in Wichita for 120 Days

A comparison of the predicted and measured high wind-speed values showed that the global trend of the predicted values captured the measured values with slightly less reliability than the mean values (Figure 6.4 and Figure 6.5). For example, some high wind-speed points were evident in all year groups due to high wind-speed values in the corner cities, which represent single-peak measurements. However, the interpolated values represented the weighted average values for all the high measurements in the four corner cities at any given time, but the mean wind-

speed values represent the average daily wind-speed readings. Because wind speed is highly affected by location and is more variable over short distances, this variation is expected to diminish if a denser network of sampled sites is available, leading to accurate and precise interpolated values. Table 6.1 and Table 6.2 compare high and mean wind speeds, respectively, for Wichita, using minimum, maximum, average, standard deviation, root mean square error (RMSE), and mean error (ME).

$$RMSE = \sqrt{\frac{1}{N}\sum_{1}^{N}[\acute{Z}\,(x_\circ, y_\circ)_i - Z\,(x_\circ, y_\circ)_i]^2}$$

Equation 6.1

$$ME = \frac{1}{N}\sum_{1}^{N}[\acute{Z}\,(x_\circ, y_\circ)_i - Z\,(x_\circ, y_\circ)_i]$$

Equation 6.2

Where:

$\acute{Z}\,(x_\circ, y_\circ)$ is the predicated value at a certain location $(x_\circ, y_\circ)$, and

$Z(x_i, y_i)$ is the measured value at the sample point (x_i, y_i).

Table 6.1: Measured vs. Predicted High Wind Speeds in Wichita

Year group	Measured high				Predicted high				RMSE	ME
	Min	Max	Average	Standard deviation	Min	Max	Average	Standard deviation		
1975-1979	9	63	20	7	10.1	30.2	19.5	3.9	5.6	-0.7
1980-1984	7	47	21	7	10.1	48.0	19.4	4.8	5.2	-1.7
1985-1989	7	41	20	5	8.6	48.2	19.1	4.6	3.5	3.5
1990-1994	9	34	21	5	9.8	35.1	19.3	4.3	4.1	-1.8
1995-1999	8	43	19	6	10.7	32.0	17.9	4.4	5.5	-0.9
2000-2004	7	41	19	6	8.6	33.1	18.9	5.3	4.4	-0.5
2005-2009	6	40	21	7	7.6	35.1	18.6	5.3	5.0	-2.2
2010-2014	8	45	23	8	8.7	36.2	20.1	6.2	6.1	-3.2
2015-2019	10	48	23	7	9.6	39.3	20.7	5.9	5.8	-2.3

Table 6.2: Measured vs. Predicted Mean Wind Speeds in Wichita

Year group	Measured mean				Predicted mean				RMSE	ME
	Min	Max	Average	Standard deviation	Min	Max	Average	Standard deviation		
1975-1979	4	25	11.44	4.51	6.05	18.72	12.21	2.63	3.83	0.77
1980-1984	4	24	11.82	4.18	4.80	20.77	11.43	3.32	2.36	-0.38
1985-1989	4	24	11.44	4.00	4.36	22.18	12.22	3.25	3.38	3.38
1990-1994	4	22	12.12	3.86	5.10	21.12	12.03	3.29	2.29	-0.10
1995-1999	2	20	10.16	3.87	5.90	20.66	10.66	3.17	2.68	0.71
2000-2004	3	23	10.80	4.07	4.22	22.05	10.56	3.33	2.63	-0.24
2005-2009	1	22	10.72	4.41	1.97	17.96	9.99	3.34	2.58	-0.73
2010-2014	3	29	11.52	5.34	3.33	23.35	10.33	4.00	2.87	-1.20
2015-2019	4	22	11.42	4.07	4.02	20.32	10.69	3.46	2.32	-0.72

The Chi-square goodness of fit test is a hypothesis testing method that assesses the goodness of fit and measures the significant difference between observed values and theoretical values to determine whether or not the sample data matches the population. In other words, the test shows how well the sample data fits a set of observations. To assess the goodness of fit of the interpolated wind-speed values and how close these values align with the measured values, the null hypothesis H_0, stated as $(V_i)_{Predicted} = (V_i)_{Measured}$, and the alternate hypothesis, H_1, stated that some predicted mean and high wind speeds differed from measured values. The level of significance was chosen as $\alpha = 0.05$ based on engineering judgment and evaluation of the degree of freedom, meaning the critical value could be calculated from the Chi-distribution, resulting in 146.6, as shown in Figure 6.6. Then the value of the test was calculated based on Equation 6.3. If χ^2 is less than the critical value, then null hypothesis H_0 should be accepted, otherwise H_0 should be rejected.

$$\chi^2 = \sum \frac{(O - E)^2}{E}$$

Equation 6.3

Where:

O represents observed values, and

E represents expected values.

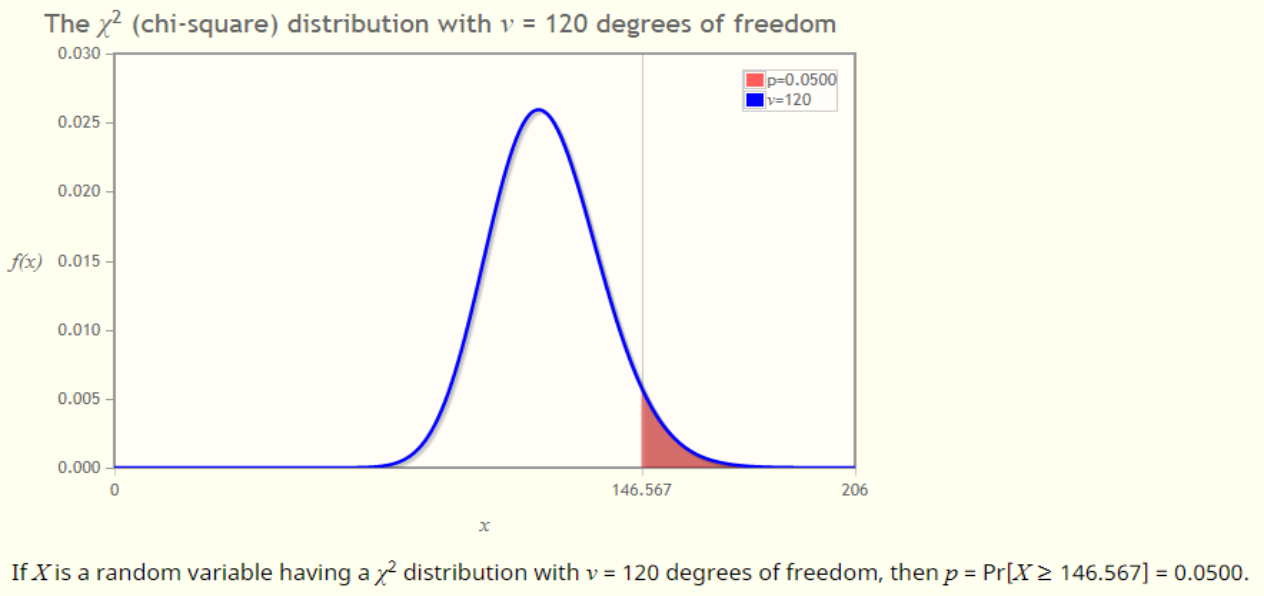

Figure 6.6: Critical Chi-Square Value

Table 6.3 presents the Chi-square goodness of fit test analysis results used to determine effective prediction. Decision-rule results revealed that, although mean wind-speed prediction was acceptable according to Chi-square for all year groups, high wind speed was only acceptable for three of the year groups (1985–1989, 1990–1994, and 2000–2004) and rejected for the rest of the groups. This does not mean, however, that the predicted high wind speed did not reflect the measured values; as stated, high wind speeds show that high peaks could not be recovered exactly from the corner cities.

Moreover, the decisions were made at 95% confidence level ($\alpha = 0.05$), which is considered a tight criterion for recovering high wind speeds, so it is unreliable to state that the interpolated wind speeds do not represent the measured speeds. A more precise result could be achieved by refining the interpolation mesh to recover exact values. Results also may differ slightly because wind-speed measurements may be taken at specific locations in the cities, but the interpolation method assumes a central coordinate of the cities. However, if sufficient data is lacking, this method can accurately predict wind speeds.

Table 6.3: Chi-Square Goodness of Fit Results

Year group	High wind speed			Mean wind speed		
	χ^2	$\chi^2_{,Df,\alpha}$	Decision	χ^2	$\chi^2_{,Df,\alpha}$	Decision
1975-1979	179.88	146.6	Reject	146.34	146.6	Accept
1980-1984	164.06	146.6	Reject	63.71	146.6	Accept
1985-1989	113.96	146.6	Accept	76.80	146.6	Accept
1990-1994	111.28	146.6	Accept	59.08	146.6	Accept
1995-1999	237.17	146.6	Reject	89.27	146.6	Accept
2000-2004	120.01	146.6	Accept	82.41	146.6	Accept
2005-2009	166.04	146.6	Reject	104.48	146.6	Accept
2010-2014	250.54	146.6	Reject	110.21	146.6	Accept
2015-2019	219.54	146.6	Reject	67.71	146.6	Accept

The goodness of fit assessment, which was made for the entire year in all year groups, may be unrealistic because the FE interpolation technique is easily affected by uneven distribution of observational data points since the same weight is assigned to each city regardless of the season. In the winter, even though the high wind-speed measurements drastically change from one location to another, the weights are similar and assume even contributions. A more reliable assessment of the interpolated data should be conducted on a seasonal basis to determine the season that drives the overall behavior of the interpolated high wind-speed data to fail. Table 6.4 shows the Chi-square test results for high wind speeds for the four seasons in 1975. As expected, this method produced biased estimates in the winter, and the test failed in the winter due to the high daily variation in wind speed in the interpolated cities. However, test results were acceptable in the rest of the seasons.

Table 6.4: Chi-Square Goodness of Fit Results for 1975

Season	High wind speed		
	χ^2	$\chi^2_{,Df,\alpha}$	Decision
Winter	87.50	43.8	Reject
Spring	27.58	43.8	Accept
Summer	21.14	43.8	Accept
Autumn	43.65	43.8	Accept

Needed functional validation and assessment of the interpolated values were done by comparing the resulting values against a county's known measured wind speeds. A deep online search found mean and high wind-speed records for Sedgwick County (January 1975–2015) in the online Farmer's Almanac (https://www.almanac.com/weather/history/KS/Sedgwick/1975-01-01#). Sedgwick County, which is in Zone 10, is bounded by Wichita, Chanute, Topeka, and Manhattan, with Wichita being the closest city. Table 6.5 through Table 6.13 and Figure 6.7 through Figure 6.9 compare the county's measured and predicted high and mean wind speeds for 1975–2015. Overall, the global trend of predicted values captured the measured values, but presented relatively higher peak-speed values for the year 1990, lower values in years 2000 and 2005, and nearly identical values for the rest of the years. Based on the interpolation technique, the closest city to the interpolated city has a significant contribution; therefore, Wichita had the most significant effect on the interpolated values (higher weight function). Compared to 2000 and 2005, higher values were observed in 1990 because Wichita has higher values in 1990 than 2000 and 2005. Adequate care should be given during the meshing of the study area since it is a highly spatially dependent interpolator.

Table 6.5: Measured vs. Predicted Wind Speeds in 1975

Year 1975	Measured values (mph)		Interpolated values (mph)	
Day	Medium	High	Medium	High
1-Jan	7.94	13.81	6.97	12.06
2-Jan	10.93	21.86	9.99	21.87
3-Jan	13.12	19.68	13.83	19.92
4-Jan	6.67	10.24	5.97	11.92
5-Jan	17.61	26.35	18.88	25.95
6-Jan	11.39	23.02	8.89	14.14
7-Jan	8.52	13.81	7.99	14.01
8-Jan	10.7	26.35	12.84	25.53
9-Jan	18.53	25.32	19.85	24.97
10-Jan	22.21	63.29	24.72	61.95
11-Jan	18.41	27.73	15.96	22.93
12-Jan	14.15	20.83	13.81	20.85
13-Jan	10.01	18.3	9.10	18.14
14-Jan	9.32	17.26	8.02	17.10
15-Jan	5.41	11.62	6.98	24.69
16-Jan	14.15	25.32	13.78	20.75
17-Jan	7.71	16.11	8.02	16.02
18-Jan	7.61	14.96	7.06	14.91
19-Jan	17.95	34.64	18.90	33.67
20-Jan	14.85	27.73	13.96	27.79
21-Jan	17.15	27.73	15.05	27.79
22-Jan	10.93	21.86	10.87	20.78
23-Jan	12.2	20.83	12.03	21.00
24-Jan	16.69	27.73	14.95	27.77
25-Jan	13	23.02	11.14	23.18
26-Jan	9.32	20.38	8.97	20.89
27-Jan	15.19	26.35	14.91	25.79
28-Jan	12.43	20.83	11.90	20.85
29-Jan	15.88	25.32	14.93	24.81
30-Jan	6.44	11.62	9.01	19.95
31-Jan	14.27	19.68	14.91	19.93

Table 6.6: Measured vs. Predicted Wind Speeds in 1980

Year 1980	Measured values (mph)		Interpolated values (mph)	
Day	Medium	High	Medium	High
1-Jan	4.72	8.06	4.94	9.03
2-Jan	8.86	17.26	9.90	21.79
3-Jan	13.81	21.86	12.85	19.75
4-Jan	6.1	10.24	5.94	10.05
5-Jan	9.32	17.26	9.86	17.00
6-Jan	20.37	29.92	22.79	29.77
7-Jan	15.19	27.73	13.81	20.77
8-Jan	8.63	18.3	7.01	17.84
9-Jan	9.55	13.81	10.96	14.96
10-Jan	23.02	38.79	23.96	35.89
11-Jan	19.68	31.07	18.84	30.61
12-Jan	16.34	32.22	16.86	31.91
13-Jan	18.07	26.35	16.88	25.88
14-Jan	9.09	20.83	9.88	28.61
15-Jan	17.84	28.88	17.72	27.71
16-Jan	15.08	23.02	15.00	22.99
17-Jan	6.44	18.3	4.97	7.07
18-Jan	7.48	16.11	6.89	16.86
19-Jan	12.08	21.86	12.02	21.90
20-Jan	13.81	21.86	11.94	18.02
21-Jan	8.17	17.26	7.04	17.00
22-Jan	15.88	20.83	15.99	21.08
23-Jan	10.7	17.26	9.95	17.04
24-Jan	10.01	13.81	10.04	14.12
25-Jan	11.16	17.26	12.89	22.93
26-Jan	20.94	24.17	21.81	23.85
27-Jan	14.15	19.68	14.86	17.95
28-Jan	12.77	17.26	12.91	19.88
29-Jan	14.27	19.68	14.83	18.02
30-Jan	15.54	25.32	13.95	24.79
31-Jan	10.36	17.26	9.92	15.85

Table 6.7: Measured vs. Predicted Wind Speeds in 1985

Year 1985	Measured values (mph)		Interpolated values (mph)	
Day	Medium	High	Medium	High
1-Jan	15.31	18.3	13.95	17.98
2-Jan	6.1	11.62	4.95	11.95
3-Jan	4.6	8.06	3.94	7.01
4-Jan	8.75	19.68	8.95	19.88
5-Jan	10.7	19.68	9.93	14.96
6-Jan	9.44	17.26	10.01	16.99
7-Jan	11.05	16.11	9.98	15.95
8-Jan	8.75	18.3	9.00	17.84
9-Jan	15.65	23.02	14.85	22.75
10-Jan	13.23	20.83	13.85	20.78
11-Jan	13.81	20.83	13.99	20.99
12-Jan	10.93	16.11	10.86	15.94
13-Jan	11.97	18.3	11.99	18.08
14-Jan	14.15	20.83	12.98	20.88
15-Jan	12.89	25.32	10.94	25.63
16-Jan	13.23	24.17	10.02	24.01
17-Jan	9.09	14.96	9.05	15.13
18-Jan	11.28	17.26	12.05	17.10
19-Jan	14.61	32.22	16.04	31.77
20-Jan	20.83	28.88	18.76	25.75
21-Jan	11.16	16.11	9.98	16.08
22-Jan	9.44	13.81	8.88	11.96
23-Jan	8.4	14.96	8.02	15.07
24-Jan	12.43	24.17	12.02	23.85
25-Jan	14.96	28.88	14.06	28.82
26-Jan	13	27.73	11.91	27.69
27-Jan	10.01	16.11	6.99	15.90
28-Jan	8.17	11.62	7.83	12.88
29-Jan	11.16	17.26	11.85	16.86
30-Jan	16.46	28.88	17.05	29.91
31-Jan	19.79	29.92	18.72	25.67

Table 6.8: Measured vs. Predicted Wind Speeds in 1990

Year 1990	Measured values (mph)		Interpolated values (mph)	
Day	Medium	High	Medium	High
1-Jan	10.24	20.83	10.84	20.93
2-Jan	19.91	23.02	21.79	32.70
3-Jan	15.42	23.02	16.90	24.88
4-Jan	9.44	17.26	16.68	27.49
5-Jan	6.79	13.81	7.90	15.91
6-Jan	6.33	6.9	6.89	9.98
7-Jan	8.52	13.81	7.97	13.96
8-Jan	12.77	18.3	9.05	18.03
9-Jan	15.65	19.68	15.89	23.80
10-Jan	11.05	17.26	9.06	17.98
11-Jan	15.88	25.32	13.99	27.84
12-Jan	16.34	20.83	16.85	23.78
13-Jan	4.83	9.21	14.92	30.63
14-Jan	15.08	19.68	13.79	17.82
15-Jan	13.46	19.68	10.86	21.72
16-Jan	12.89	17.26	14.06	22.91
17-Jan	10.36	17.26	9.87	15.95
18-Jan	12.66	17.26	11.94	19.84
19-Jan	12.31	17.26	12.09	18.06
20-Jan	2.88	5.87	13.96	24.81
21-Jan	10.36	17.26	9.96	14.08
22-Jan	3.68	8.06	6.94	13.80
23-Jan	15.19	23.02	13.94	21.95
24-Jan	11.74	26.35	13.94	31.83
25-Jan	16.46	34.41	14.95	18.05
26-Jan	12.54	18.3	10.97	24.83
27-Jan	9.9	17.26	20.00	27.94
28-Jan	6.21	11.62	5.96	12.06
29-Jan	10.93	23.02	9.97	29.71
30-Jan	11.62	17.26	10.00	17.01
31-Jan	17.84	23.02	15.99	29.92

Table 6.9: Measured vs. Predicted Wind Speeds in 1995

Year 1995	Measured values (mph)		Interpolated values (mph)	
Day	Medium	High	Medium	High
1-Jan	12.54	26.35	11.95	16.97
2-Jan	4.49	9.21	5.96	11.92
3-Jan	11.39	20.6	14.87	21.85
4-Jan	5.18	11.39	5.01	12.99
5-Jan	14.27	26.35	15.90	30.76
6-Jan	18.07	26.35	17.72	28.91
7-Jan	11.28	20.6	10.87	14.95
8-Jan	8.29	12.54	9.01	14.05
9-Jan	5.52	10.24	3.01	8.99
10-Jan	5.41	8.06	5.03	8.07
11-Jan	7.25	14.73	6.03	13.07
12-Jan	7.83	19.45	5.96	14.99
13-Jan	11.16	18.3	9.98	15.99
14-Jan	8.06	12.54	8.05	13.00
15-Jan	11.74	22.79	10.94	22.85
16-Jan	19.68	28.65	18.93	24.95
17-Jan	13.81	22.79	12.92	23.76
18-Jan	4.72	9.21	5.99	11.93
19-Jan	9.09	17.26	10.02	18.11
20-Jan	6.44	12.54	6.05	14.13
21-Jan	9.67	17.26	11.01	19.92
22-Jan	6.21	19.45	8.08	18.07
23-Jan	7.02	12.54	8.95	13.03
24-Jan	8.4	11.39	6.97	12.95
25-Jan	6.79	11.39	5.95	13.93
26-Jan	10.93	19.45	10.00	16.97
27-Jan	11.74	18.3	14.92	21.87
28-Jan	20.25	25.32	19.87	25.78
29-Jan	16.46	22.79	15.89	20.84
30-Jan	5.98	14.73	4.96	8.10
31-Jan	8.86	14.73	6.08	14.03

Table 6.10: Measured vs. Predicted Wind Speeds in 2000

Year 2000	Measured values (mph)		Interpolated values (mph)	
Day	Medium	High	Medium	High
1-Jan	14.15	27.5	13.81	24.91
2-Jan	13.58	26.35	10.06	17.14
3-Jan	12.77	29.92	14.85	28.75
4-Jan	15.65	28.88	15.79	23.72
5-Jan	16.69	31.07	15.77	25.87
6-Jan	7.36	11.39	5.93	9.06
7-Jan	9.44	24.17	5.95	16.00
8-Jan	12.89	19.45	9.88	16.98
9-Jan	6.9	12.77	6.96	13.99
10-Jan	10.13	16.11	10.95	16.09
11-Jan	7.25	12.77	5.95	12.89
12-Jan	12.66	23.02	10.84	21.76
13-Jan	10.01	16.11	9.86	13.87
14-Jan	14.61	32.22	11.83	25.96
15-Jan	22.56	28.88	14.95	23.96
16-Jan	10.01	17.26	10.95	21.82
17-Jan	8.17	12.77	6.96	12.86
18-Jan	5.52	12.77	5.91	12.89
19-Jan	13.69	31.07	10.98	30.76
20-Jan	11.39	26.35	8.91	13.90
21-Jan	11.16	23.02	10.82	21.81
22-Jan	8.29	12.77	5.89	9.98
23-Jan	9.55	21.86	8.96	21.77
24-Jan	11.05	24.17	7.90	19.87
25-Jan	12.54	20.83	11.90	20.90
26-Jan	5.87	10.24	8.91	12.90
27-Jan	8.17	11.39	8.98	13.97
28-Jan	4.95	9.21	5.96	9.00
29-Jan	3.68	8.06	4.95	8.99
30-Jan	5.98	11.39	5.06	10.03
31-Jan	4.95	13.81	3.01	13.03

Table 6.11: Measured vs. Predicted Wind Speeds in 2005

Year 2005	Measured values (mph)		Interpolated values (mph)	
Day	Medium	High	Medium	High
1-Jan	14.96	28.88	1.11	7.20
2-Jan	12.89	19.45	15.73	27.82
3-Jan	3.34	12.77	12.92	16.09
4-Jan	4.9	12.9	5.11	13.16
5-Jan	9	17.1	8.92	16.87
6-Jan	3.8	13.81	9.85	17.00
7-Jan	10.13	14.96	7.82	13.79
8-Jan	7.83	18.3	3.95	7.13
9-Jan	11.62	19.45	3.98	13.05
10-Jan	9.32	11.39	9.86	14.96
11-Jan	6.79	16.11	10.85	14.93
12-Jan	3.57	21.86	7.83	11.91
13-Jan	16.8	24.17	8.88	21.84
14-Jan	10.93	14.96	15.73	21.70
15-Jan	10.82	16.11	11.78	16.20
16-Jan	7.13	10.24	11.93	15.99
17-Jan	5.75	8.06	7.04	9.17
18-Jan	22.33	28.88	5.91	8.92
19-Jan	9.78	20.83	11.62	27.24
20-Jan	9.44	13.81	6.08	14.14
21-Jan	7.36	13.81	6.95	11.95
22-Jan	20.48	32.22	6.94	14.06
23-Jan	9.09	17.26	19.59	29.51
24-Jan	6.56	11.39	11.84	22.74
25-Jan	5.75	10.24	8.95	14.05
26-Jan	10.13	16.11	4.12	13.04
27-Jan	7.94	12.77	10.91	16.84
28-Jan	7.36	10.24	10.92	13.97
29-Jan	1.61	5.87	6.95	12.92
30-Jan	1.04	5.87	2.03	6.03
31-Jan	0.69	4.72	3.01	13.03

Table 6.12: Measured vs. Predicted Wind Speeds in 2010

Year 2010	Measured values (mph)		Interpolated values (mph)	
Day	Medium	High	Medium	High
1-Jan	6.9	17.26	9.82	19.80
2-Jan	10.47	17.26	7.98	15.92
3-Jan	8.63	12.77	9.92	14.92
4-Jan	7.02	12.77	4.94	12.87
5-Jan	4.83	10.24	6.83	14.76
6-Jan	10.59	23.02	14.75	32.55
7-Jan	24.4	29.92	22.67	31.59
8-Jan	15.19	24.17	10.85	21.66
9-Jan	4.49	6.9	3.90	7.90
10-Jan	10.47	19.45	10.84	23.83
11-Jan	7.83	14.96	6.93	15.81
12-Jan	5.87	10.24	6.94	13.97
13-Jan	14.85	26.35	14.92	29.51
14-Jan	5.52	16.11	3.96	10.02
15-Jan	5.06	10.24	3.92	8.90
16-Jan	2.88	6.9	2.98	9.00
17-Jan	4.72	10.24	4.96	11.91
18-Jan	5.18	11.39	5.90	13.84
19-Jan	7.48	14.96	6.98	15.87
20-Jan	8.4	18.3	7.97	23.78
21-Jan	10.36	17.26	10.88	20.82
22-Jan	12.31	24.17	15.74	28.66
23-Jan	16	23.02	14.01	27.93
24-Jan	16.69	32.22	16.77	32.52
25-Jan	18.64	44.88	18.80	44.18
26-Jan	8.17	17.26	6.97	15.01
27-Jan	9.78	17.26	11.79	19.85
28-Jan	14.73	21.86	15.74	24.71
29-Jan	15.77	20.83	13.90	22.78
30-Jan	6.1	13.81	4.93	9.96
31-Jan	6.67	12.77	8.82	15.84

Table 6.13: Measured vs. Predicted Wind Speeds in 2015

Year 2015	Measured values (mph)		Interpolated values (mph)	
Day	Medium	High	Medium	High
1-Jan	7.71	10.24	7.95	14.05
2-Jan	5.87	11.39	5.93	13.93
3-Jan	4.37	11.39	8.86	35.50
4-Jan	18.18	34.41	12.88	36.44
5-Jan	7.94	19.68	9.85	21.87
6-Jan	9.55	19.68	8.94	24.74
7-Jan	15.54	26.35	14.86	29.73
8-Jan	13	25.32	14.95	32.81
9-Jan	13.81	25.32	10.88	25.72
10-Jan	12.43	24.17	14.90	27.99
11-Jan	12.08	17.26	8.91	17.97
12-Jan	12.43	23.02	14.88	23.89
13-Jan	8.63	17.26	6.96	14.96
14-Jan	4.95	9.21	4.93	11.93
15-Jan	6.56	17.26	5.96	16.90
16-Jan	8.4	19.68	10.92	22.03
17-Jan	15.19	31.07	13.86	32.69
18-Jan	10.7	20.83	9.86	21.90
19-Jan	7.71	16.11	6.95	21.84
20-Jan	7.25	13.81	7.91	14.94
21-Jan	7.94	10.24	6.94	12.06
22-Jan	8.52	12.77	7.86	16.78
23-Jan	6.33	16.11	7.91	17.03
24-Jan	10.47	23.02	11.89	23.88
25-Jan	20.14	33.26	18.75	37.61
26-Jan	8.75	19.68	8.92	22.77
27-Jan	7.02	16.11	8.88	17.91
28-Jan	11.51	20.83	11.92	23.04
29-Jan	17.26	24.17	14.84	35.59
30-Jan	5.18	11.39	4.93	10.04
31-Jan	8.4	18.3	10.85	17.90

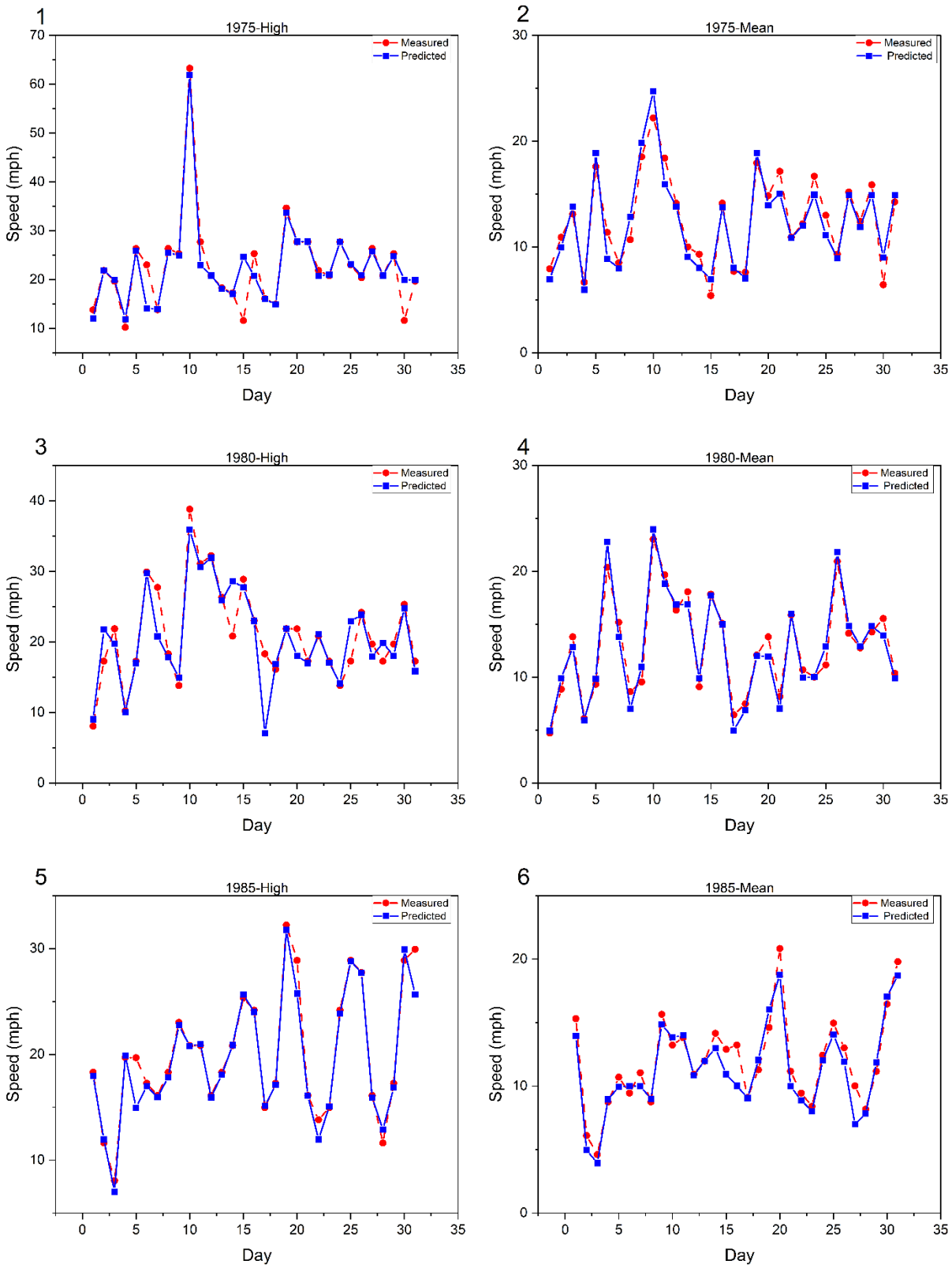

Figure 6.7: Measured vs. Predicted High and Mean Wind Speeds for Sedgwick County, 1975, 1980, 1985

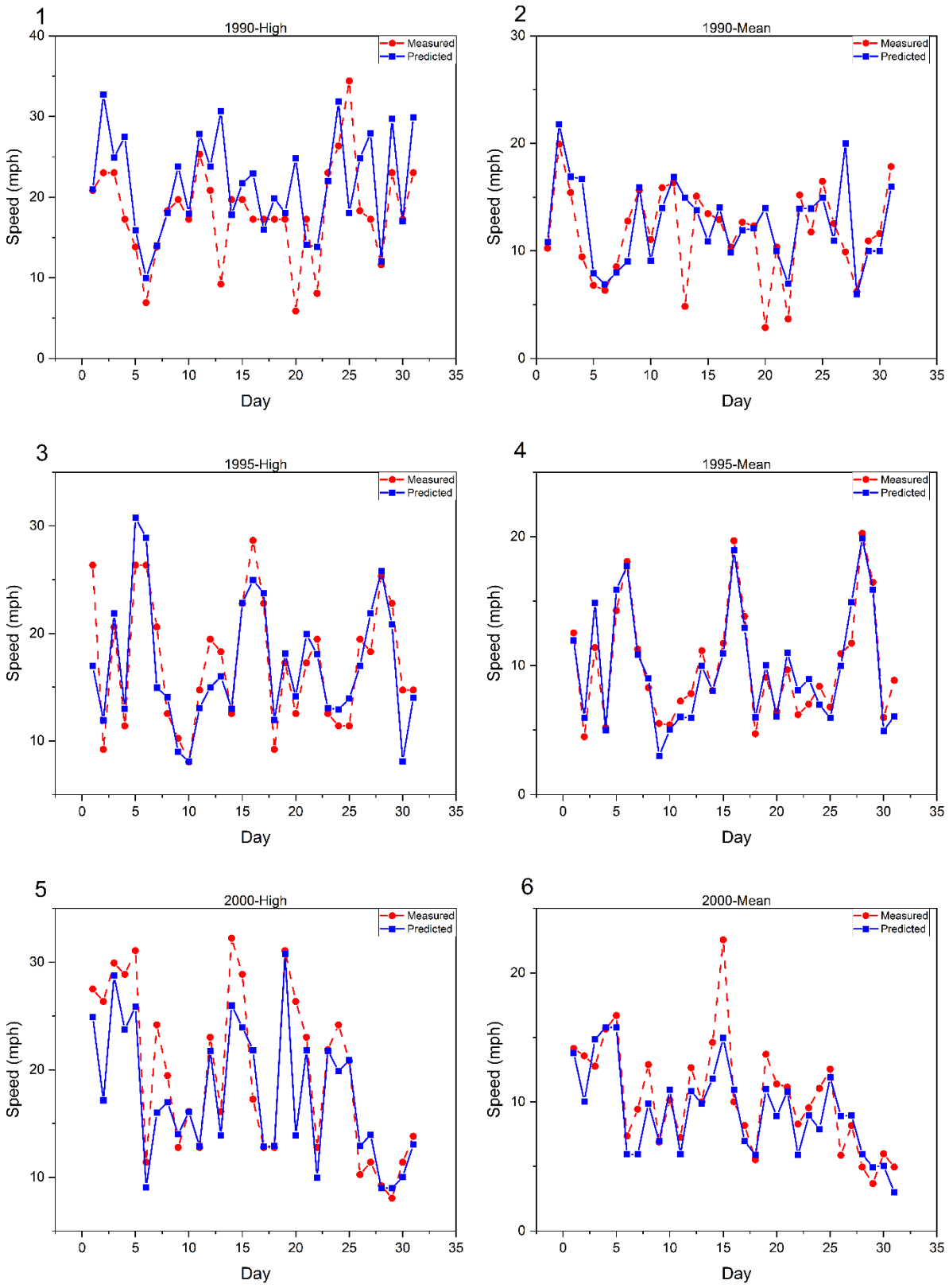

Figure 6.8: Measured vs. Predicted High and Mean Wind Speeds for Sedgwick County, 1990, 1995, 2000

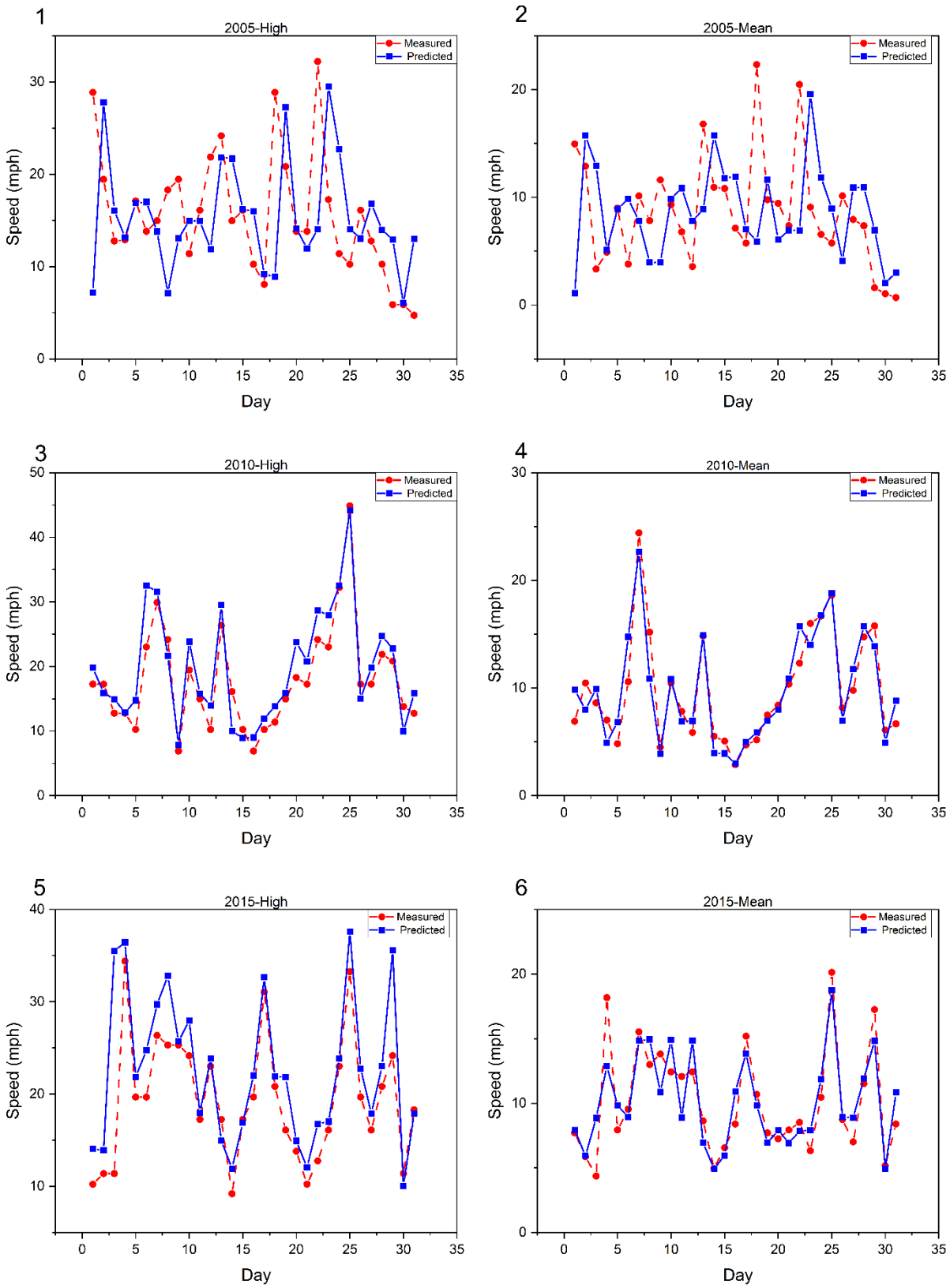

Figure 6.9: Measured vs. Predicted High and Mean Wind Speeds for Sedgwick County, 2005, 2010, 2015

6.1 Comparison of Kansas Cities

This section compares wind speed cycles for main cities in Kansas to guide the highway agency (KDOT) to prioritize their fatigue inspection plans. Comparing the corresponding number of cycles for similar wind speeds indicates the wind loading differences for any cities under investigation since higher wind cycles produce more significant fatigue damage. However, if the wind speed values differ, comparing the number of cycles provides no measure on which city would experience more damage since the fatigue damage is a function of stress and the number of cycles. Lower wind speeds with a higher number of cycles could produce damage equivalent to higher wind speeds with a lower number of cycles since the stress experienced by the structure increased with increasing wind speed. To measure the damaging effect for a wind speeds content, the wind speed and number of cycles effect should be combined to yield a representative damaging index. The damaging index depends implicitly on the wind speed and could be expressed as follows:

$$\sigma = f(V)$$

$$D = f(\sigma, N)$$

$$N_f = \frac{A}{\sigma^3}$$

$$\sigma = CV^2$$

$$D = CNV^6$$

Where:
V is the wind speed,
σ is the stress produced by wind speed,
N_f number of cycles to failure, and
D is the damaging index.

A higher damaging index indicates more significant damage in the structures in any given city. The cumulative 45-years damaging index was produced for the eight main cities in Kansas and plotted as in Figure 6.10. As indicated from the plot, the sign structures located in Dodge City and Goodland are expected to experience more damage in the 45-years period, and more in-depth investigation should be made to evaluate the structures in these cities.

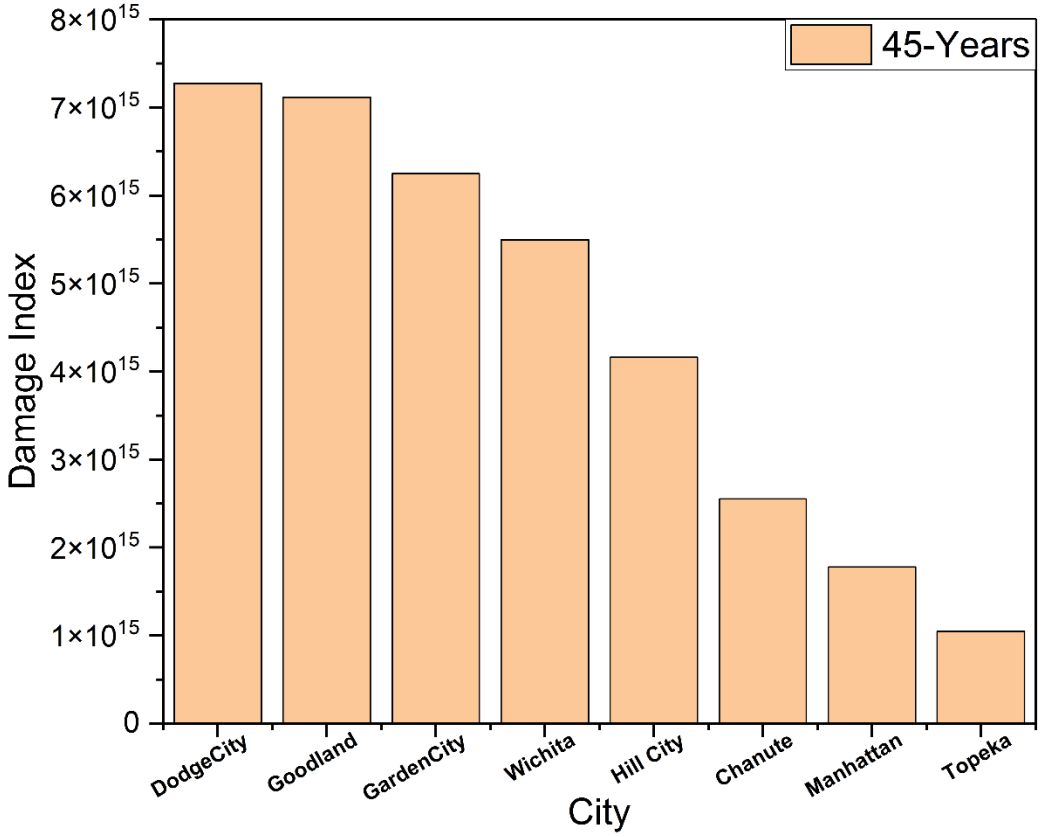

Figure 6.10: 45-Years Damaging Index for Main Cities in Kansas

The 10-years damaging index is plotted in Figure 6.11 for the main cities in Kansas from 1980-2019 to examine the period in which the higher damaging effect occurs.

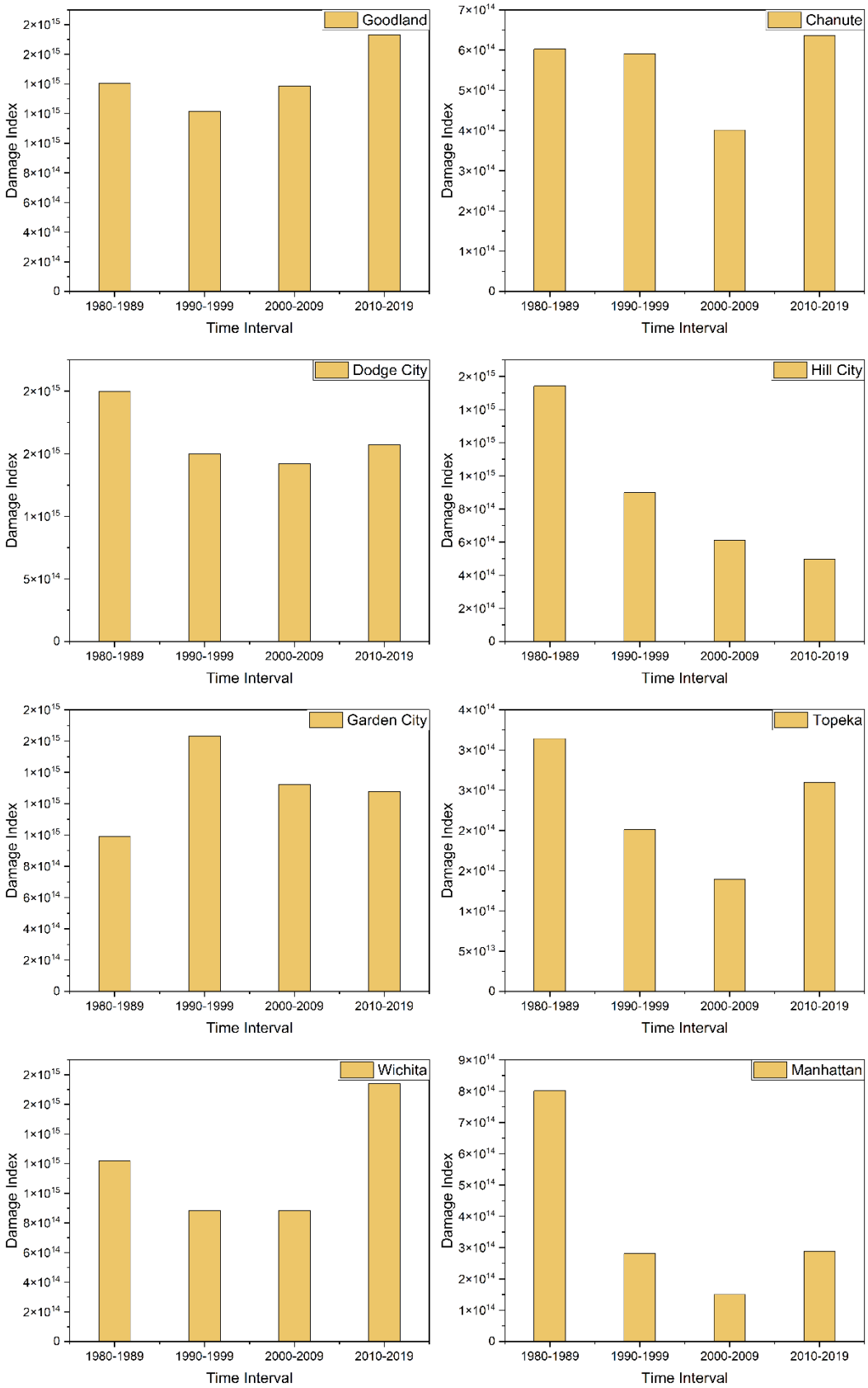

Figure 6.11: The 10-Years Damaging Index for Main Cities in Kansas

Chapter 7: Conclusions and Recommendations

This study used finite element shape functions to conduct spatial interpolation of wind-speed records for all Kansas counties. This method considered spatial correlations among boundary sites. Artificial wind-time histories were constructed for each day for the entire 45-year study period, and the number of cycles developed using Rainflow analysis was used to provide descriptive wind loading for civil engineering applications. User-friendly software was developed using C# to extrapolate wind-speed cycles for any given year in the future. The following conclusions and findings were drawn from this study:

1. The finite element spatial interpolation technique accurately estimates spatially continuous phenomena from measured values at limited sample points.
2. Adequate care should be given during the meshing of the study area in terms of the element size, since this method is highly spatially dependent.
3. The FE interpolation technique proved to be an excellent spatial interpolator for recovering Wichita records based on statistical assessment.
4. The global trend of predicted values in Sedgwick County captured the measured values and continued to commit relatively high peak wind-speed values for the year 1990 and low values in the years 2000 and 2005.
5. The number of cycles resulting from the rainflow analysis for the developed time histories was less than the number of cycles previously determined by the deterministic approach at Kansas State University, which was conservatively assumed to include dynamic amplification effects.

References

Alshareef, H. A., Rasheed, H. A., Abouelleil, A., & Al-Masri, R. (2019). *Initial analytical investigation of overhead sign trusses with respect to remaining fatigue life and predictive methods for inspection* (Report No. K-TRAN: KSU-17-4). Topeka, KS: Kansas Department of Transportation.

ASTM E1049-85. (2017). *Standard practices for cycle counting in fatigue analysis*. West Conshohocken, PA: ASTM International. doi: 10.1520/E1049-85R17, www.astm.org

Cochran, L. (2012). Chapter 1: Wind issues in the design of buildings. In *Wind issues in the design of buildings* (pp. 1–16). https://doi.org/10.1061/9780784412251.ch01

Davenport, A. G. (1962). The spectrum of horizontal gustiness near the ground in high winds. *Quarterly Journal of the Royal Meteorological Society, 88*(376), 197–198. https://doi.org/10.1002/qj.49708837618

Ginal, S. (2003). *Fatigue performance of full-span sign support structures considering truck-induced gust and natural wind pressure* [Master's thesis]. Marquette University.

Iannuzzi, A., & Spinelli, P. (1987). Artificial wind generation and structural response. *Journal of Structural Engineering, 113*(12), 2382–2398. https://doi.org/10.1061/(ASCE)0733-9445(1987)113:12(2382)

Kaimal, J. C., Wyngaard, J. C., Izumi, Y., & Coté, O. R. (1972). Spectral characteristics of surface-layer turbulence. *Quarterly Journal of the Royal Meteorological Society, 98*(417), 563–589. https://doi.org/10.1002/qj.49709841707

Kattan, P. I. (2003). *MATLAB guide to finite elements: An interactive approach*. https://doi.org/10.1007/978-3-662-05209-9

Luo, W., Taylor, M. C., & Parker, S. R. (2008). A comparison of spatial interpolation methods to estimate continuous wind speed surfaces using irregularly distributed data from England and Wales. *International Journal of Climatology, 28*(7), 947–959. https://doi.org/10.1002/joc.1583

Matsuishi, M., & Endo, T. (1968). *Fatigue of metals subjected to varying stress*. Presented to the Japan Society of Mechanical Engineers, Fukuoka, Japan.

Webster, R., & Oliver, M. A. (2007). *Geostatistics for environmental scientists* (2nd ed.). Hoboken, NJ: John Wiley & Sons.

K-TRAN

KANSAS TRANSPORTATION RESEARCH AND NEW-DEVELOPMENT PROGRAM

AD ASTRA PER ASPERA

Kansas

Department of Transportation